A NEW RELIABILITY ASSESSMENT MODEL FOR POWER ELECTRONIC MODULES CONSIDERING FAILURE MECHANISM INTERACTION

A Thesis
Submitted to the Graduate Faculty
of the
North Dakota State University
of Agriculture and Applied Science

By

Xing Zhuang

In Partial Fulfillment of the Requirements
for the Degree of
MASTER OF SCIENCE

Major Program:
Industrial Engineering and Management

November 2015

Fargo, North Dakota

North Dakota State University
Graduate School

Title

A NEW RELIABILITY ASSESSMENT MODEL FOR POWER ELECTRONIC MODULES CONSIDERING FAILURE MECHANISM INTERACTION

By

XING ZHUANG

The Supervisory Committee certifies that this ***disquisition*** complies with North Dakota State University's regulations and meets the accepted standards for the degree of

MASTER OF SCIENCE

SUPERVISORY COMMITTEE:

Om Prakash Yadav
Chair

Akm Bashir Khoda

Benjamin Braaten

Brij Singh

Approved:

11/16/2015
Date

Om Prakash Yadav
Department Chair

ABSTRACT

A reliability prediction method is proposed to determine the lifetime of IGBTs (Insulated Gate Bipolar Transistors) under power cycling test based on the performance of solder joint and wire bond. The failure characteristics of solder joint and wire bond are captured via selected PoF model respectively. To provide precise reliability prediction, PoF models are converted into probabilistic models. In addition, the failure interaction between wire bond and solder joint is studied. Wire bond lift-off is treated as the predominant failure mode based upon experiments from literature and solder joint degradation process is triggered by wire bond degradation process. Increased junction temperature is captured as it is affected by the degradation process of both components. In the end, the system reliability is computed in a series system configuration.

ACKNOWLEDGEMENTS

I am very thankful to my advisor and committee chair, Dr. Om Yadav, for offering his time, guidance, support and help throughout my study. His valuable suggestions and persistent help make this research work a possibility.

I would like to thank my family, especially my parents, for their enlightenment, support and encouragement.

I also want to acknowledge my colleague, Shah Limon, who provided me with a lot of help and knowledge for this study.

Last but not least, I would like to thank Dr. Brij Singh, Dr. Bashir Khoda and Dr. Benjamin Braaten for their diligent guide and support for my research.

TABLE OF CONTENTS

ABSTRACT iii

ACKNOWLEDGEMENTS iv

LIST OF TABLES vii

LIST OF FIGURES viii

1. INTRODUCTION 1

  1.1. Importance of the Research Studies 1

  1.2. Research Motivation 2

  1.3. Research Approach/Methodology 5

    1.3.1. Literature Review 5

    1.3.2. Proposed Reliability Model 6

    1.3.3. Data Collecting Method 6

    1.3.4. Data Analysis and Interpretation Strategies 7

    1.3.5. Reliability Analysis and Discussion 7

  1.4. Organization of the Thesis 7

2. LITERATURE REVIEW 9

  2.1. Introduction 9

  2.2. Part-count Reliability Model 9

  2.3. System-level Reliability Model 11

    2.3.1. Reliability Block Diagram 11

    2.3.2. Degradation Modeling 12

    2.3.3. Competing Failure Mode and Related Derivatives 14

  2.4. Bayesian Model Averaging 16

  2.5. Physics of Failure Modeling 18

    2.5.1. Wire Bond Lift-off 18

2.5.2. Solder Joint Delamination 25

3. PROPOSED RELIABILITY MODEL 29

3.1. Initial PoF Models Selection 29

3.1.1. Solder Joint PoF Model 29

3.1.2. Wire Bond PoF Model 30

3.2. Probabilistic Modeling 31

3.3. Modeling Component Failure Mechanism Interaction 33

3.4. System Reliability Modeling 40

4. EXAMPLE 43

4.1. Background 43

4.2. Data Collection 44

4.3. Data Development 44

4.3.1. Component Material Parameters 44

4.3.2. V_{CE} and V_{GE} Measurement 45

4.4. Data Processing and Reliability Analysis 47

5. CONCLUSION 54

REFERENCES 57

LIST OF TABLES

Table Page

1. General Degradation Data Form. 13

2. CTEs of Wires and Chips at Various Temperatures. 22

3. Elastic-plastic Change of Aluminum at Various Temperatures. 22

4. Component Parameters Summary. 45

LIST OF FIGURES

Figure		Page
1.	A reliability block diagram.	12
2.	Degradation distribution pattern.	13
3.	The thermal model of the Al-Si interface heating up.	19
4.	Crack propagates above the interface of Al-Si film.	20
5.	Wire bond interface after fatigue.	20
6.	Geometry change of model of wire bond.	21
7.	Shear force v.s. sheared area.	23
8.	Number of cycles to failure v.s. ΔT and T_m.	25
9.	Accumulative fatigue phenomenon of solder joint.	25
10.	Crack lengths of different solder heights after 450 thermal cycles.	27
11.	Probabilistic interpretation between ΔT and N_f.	32
12.	Junction temperature values versus the number of cycles.	34
13.	V_{CE} increases versus the number of cycles.	35
14.	Relative change of V_{GE} versus the number of cycles.	36
15.	Change of ΔV_{GE} in solder joint.	37
16.	Behavior of thermal resistance.	39
17.	V_{CE} value versus number of cycles.	46
18.	Increasing pattern of junction temperature during power cycling.	48
19.	Component reliability and system reliability.	51

1. INTRODUCTION

1.1. Importance of the Research Studies

Reliability assessment can provide an in-depth basis for evaluating component/system reliability during the early stages of product development. An effective reliability assessment assists in determining product reliability requirements and provides supports for reliability allocation before the design has been moved for building prototype phase.

Nowadays, components/systems are designed to function in variable stress environments. The failure of a component/system can be caused by either component self-degradation or component failure mechanism interaction. To determine the cause of failure and the behavior of system failure mechanism become difficult due to the complexity of modern system and the interrelationship among components. Reliability assessment allows companies and engineers to populate the system failure behavior with component material science and component failure mechanism interaction. This requires thorough study of system failure behavior and effective reliability and failure analysis of the system under consideration.

Recently, power electronic modules (PEMs) are widely used in energy, automotive, and aerospace industries. The PEM plays a key role in converting and controlling electrical power which leads to the need for these power electronic systems to be performing in various harsh environments and conditions. The stable performance of these applications strongly relies on the reliability of PEM. Thus, it is important to have robust failure analysis and effective reliability prediction approaches in place.

The performance of PEM-based application, such as hybrid electrical vehicles and wind turbines, is affected if the reliability assessment is not precise. This will cause chance-effect to the incorrect maintenance scheduling which leads to high warranty cost and the loss of

potentially customers and market share. For a sense of designing a system, it is important to find out a way to predict the system reliability with the performance of the critical components be estimated at any given time.

Hence, the interest of creating a method of reliability prediction on IGBT is further enhanced. A practical reliability assessment model is required to predict more accurate reliability of PEMs. Therefore, PEMs are studied insightfully as the critical component of the system and failure behavior is investigated. The further improvements on system design and quality can be practiced with quality engineering tools.

1.2. Research Motivation

Power electronic modules are operated for the purpose of controlling and converting the electrical power such as the conversion of AC to DC voltage. Also, the development of the renewable energy area is highly depending upon the functionality of the PEM, making reliability and durability of the PEM as critical requirements. Therefore, the objective of this work is to predict the PEMs system reliability in a way of encompassing the component degradation and considering interaction between existing failure mechanisms.

Several challenges have been encountered that limit the accuracy and practicality of reliability prediction for PEMs [1]. Among those challenges, the biggest challenge for PEMs-based application is to capture the failure rate of the system at any given time.

Early in the design stage, standard handbook-based models, such as military handbook MIL-HDBK-217F [2], are heavily used for reliability prediction. These handbook-based models provide a database for predicting component failure rates. However, the result is often inaccurate and misleading because these models assume component failure rates are constant. Moreover,

the failure mode and its corresponding root causes remain unidentified. Further, the variation of temperature amplitude and material properties are not considered in these models.

Later, when field failure data became available, the statistical methods are often applied to capture the component failure behavior. The traditional statistical methods fit the acquired data into a statistical model considering the failure data follow a probabilistic distribution. According to the component failure characteristic behaviors, the reliability in accordance with time is calculated and a probabilistic decreasing trend is observed [3]. Later Coit et al. [4] suggested an approach with competing failure modes to provide system reliability. The failure mechanisms are treated as independent and reliability is computed as the product of the reliability of the corresponding components. The degradation modeling seems promising at prediction system reliability. However, it relies on the availability and the representative of massive field data. Furthermore, the transformation from data to statistical modeling might lead to complexity.

Therefore, to accurately predict the reliability of PEMs, a new approach is needed for overcoming the disadvantages of the overreliance on standard handbook-based models and requirement of massive data for degradation modeling.

Additionally, the change in component material property was observed and studied for PEM-based applications. Thermo-mechanical stress induced by the mismatch of coefficient of thermal expansion (CTE) during the operation period is the major cause for PEMs' failure. Using insulated gate bipolar transistors (IGBTs) as an example in this work, it was found that wire bond and solder joint are repetitively exposed to thermo-mechanical stress [5][6], which accelerates components' fatigue failure behavior due to the change in grain size of wire bond and the slower heat dissipation of solder joint. It is evident that the wire bond lift-off process during

power cycling and the solder joint delamination accelerated by the slower heat dissipation are the main causes of system degradation and hence affect the system reliability. As a result, wire bond lift-off and solder joint delamination are the main failure mechanisms on IGBT degradation process studied in this work.

Numerous methods with different perspective of views for PEM degradation process have been used to analyze the component lifetime, such as finite elements technique [7]. Ultimately, physics-of-failure (PoF) models have been developed to provide the insightful relationship between numbers of cycle to fail and factors associated with component lifetime based on the module design. Consequently, the expected lifetime cycle for each component is estimated. Most of PoF models are developed based on Coffin-Manson and modified Coffin-Manson models to explain the component fatigue failure phenomenon. However, the lack of ability to provide proper probabilistic prediction on the reliability of wire bond and solder joint limits the applicability of PoF models. There needs to be a probabilistic approach to convert the fatigue damage into probabilistic modeling.

Lately, Advani and Yadav [8] provided a model that captures the failure of solder joint via dividing the failure process into crack initiation and propagation phases. This approach details the failure process of solder joint delamination as the power cycling preceded, but fails to combine with other components' failure behavior to provide reliability prediction on a system level. In order to provide realistic system reliability estimate, the potential failure interaction needs to be considered as one component's failure mechanism might trigger or accelerate the other's failure degradation. Work done by [9] pointed out that the failure mechanism of wire bond and solder joint were identified as the main failure mechanism for different temperature amplitude repetitively. However, these two failure mechanisms could occur simultaneously

under certain temperature amplitude. Work done by [10] stated that the predominance of wire bond lift-off was observed in the temperature amplitude ranged under 120K and the predominance of solder joint delamination beyond. In this case, the interaction of these two failure mechanisms needs to be clearly interpreted and considered to provide accurate reliability prediction for PEMs.

Therefore, in the proposed work, the failure interaction between wire bond and solder joint is identified and considered in system reliability prediction. Furthermore, the operating condition and the material properties of wire bond and solder joint are taken into account for accurate reliability prediction. This work also considers the probabilistic failure phenomena of wire bond and solder joint especially the order of the failure occurrence to provides better reliability analysis tool to predict the IGBT degradation behavior.

1.3. Research Approach/Methodology

A detailed research plan is developed in this section. Each step of the plan is structured and listed as follow.

1.3.1. Literature Review

A comprehensive summary of literature review is carried out for the foundation of this work. The reliability prediction method is entailed as the lifetime models on IGBTs component as well as system levels. The literature covers the empirical-based methods which provide reliability references at early design stage. Then, the publications that provide reliability estimate based on experiment data are included. In addition, the PoF models, which considers main factors affecting component lifetime, reviewed that provide the foundational basis for the understanding of failure mechanism on IGBTs.

The purpose of this Literature review section is to establish the basic understanding of reliability prediction approaches, study the component/system failure mechanism and determine the interrelationship between wire bond and solder joint. Upon this point, a clear sequence of thoughts on modeling the system reliability with respect to time and critical parameters are developed.

1.3.2. Proposed Reliability Model

After identifying research problem, the new reliability prediction model is proposed. The main failure mechanisms are studied and considered in the proposal reliability model. The temperature variation that IGBT undergoes is found to be the root cause of the degradation process. According to PoF models, the component lifetime is determined if the temperature amplitude and the physical dimension of the wire bond and solder joint are set. Therefore, the PoF models are selected for each of the components based upon the coverage of physical attributes and the working conditions.

The increased pattern of voltage for collector-emitter (V_{CE}) and gate-emitter (V_{GE}) are the indicators for fatigue degrees for wire bond and solder joint respectively. The failure behavior of wire bond and solder joint is interpreted via monitoring V_{CE} and V_{GE} with regression technique.

In addition, the failure interaction between solder joint and wire bond has been studied with literature pointing out that wire bond lift-off is dominant failure mechanism. The solder joint degradation process is triggered by wire bond lift-off phenomenon that represents the case of failure mechanism interaction and hence modeled in the proposed work.

1.3.3. Data Collecting Method

After defining the model in previous step, the data needed for the proposed reliability model were collected from the several literature [6] [22] [34], where proper experiments were set

up to achieve designated conditions to monitor IGBT degradation process. A simplified version of A IGBT specimen is used for the experiment. It often consists of wires connected to a silicon chip, which is glued adhesive to a substrate with solder joints. The whole specimen is then mounted on a water cooler [34]. From the literature where the data were cited, an IGBT module is running for a power cycling testing in a pre-defined temperature amplitude. Typically, specific current is constantly loaded and applied to the IGBT module to obtain the pre-set temperature amplitude [6] [22]. Temperature sensors are even used in [6] to monitor the change of temperature amplitude to ensure the accuracy. During the power cycling testing, the value of component failure characteristics, V_{CE} and V_{GE}, were obtained at each specific cycle from the relative literature and plotted. With all the data found and cited from literature, the data analysis is advanced.

1.3.4. Data Analysis and Interpretation Strategies

All the data collected from literature are used in the model equations to interpret the component lifetime and the failure interaction. The order of failure mechanism occurrence is demonstrated by estimating the failure behavior of wire bond and solder joint.

1.3.5. Reliability Analysis and Discussion

The model discussed above predicts the probability of PEM fails at the given cycle. In order to evaluate the effectiveness of the proposed reliability model, the result is compared to the approach without considering the failure interaction among components. Further discussion is drawn as well.

1.4. Organization of the Thesis

The remainder of the thesis is organized as follows. In Chapter 2, a literature review of the existing studies is provided. In Chapter 3, a new reliability prediction method is proposed. An

example is included in Chapter 4, in order to show the set-up of data collection and demonstrate the performance and effectiveness of the proposed reliability prediction model. Reliability analysis based on the proposed reliability prediction model is developed in Chapter 5. At last, the conclusion is drawn in Chapter 6.

2. LITERATURE REVIEW

2.1. Introduction

This chapter focuses on the contributions from existing literature to develop the concepts upon modeling the reliability of the IGBT module and its related components. These methods and models are built considering either the failure mechanism, the corresponding material properties, the major factors causing the degradation phenomenon, or the possible correlation among components. An important take-away from this Literature Review section is that while the vast literature reviewed the most possible ways to model the module reliability, the models do not successfully combine those aspects together to lead an accurate and practical reliability prediction. The subsequent sections address the related work conducted on these methods/models

2.2. Part-count Reliability Model

The part count-reliability model is an empirical-based model due to the relative unavailability of the component performance characteristics and the system complexity at the early design stage. In this situation, a database containing field-rate data is needed as reliability references for component reliability analyses. MIL-HDBK-217 [2] is the main source as a database to demonstration component reliability. The MIL-HDBK-217 includes empirical failure rate data developed using historical information of part failure data for a large component types. The parts stress technique and the parts count technique are the main techniques in [2]. The parts stress technique requires knowledge of the stress levels on each part to determine its failure rate, while the parts count technique assumes average stress levels as a means for providing an estimate of the failure rate at early design stage. Covering 14 separate operational environments, such as ground fixed, airborne inhabited, typical factors used in determining a part's failure rate including a temperature factor (π_T), power factor (π_P), power stress factor (π_S), quality factor (π_Q)

and environmental factor (π_E) in addition to the base failure rate (λ_b). For example, the model for a resistor is as follows:

$$\lambda_{Resistor} = \lambda_b \times \pi_T \times \pi_S \times \pi_P \times \pi_Q \times \pi_E \quad (1)$$

Bellcore's [11] approach was a primary approach on telecommunications data. Similarly to MIL-HDBK-217 [2], it covers separate use environments with a prediction of an exponential failure distribution. But the reliability indices is presented as failures per billion part operating hours (FIT). Three categories are classified into: parts count approach, modification with lab test data, and field failure tracking. With these three categories, the infant mortality and the level of previous burn-in the part or unit are considered. Depending on how the system behaves in the use environment, a Bayesian weighting procedure is performed to collect data.

Another reliability data handbook, RDF 2000 [12], was developed by the French telecommunications industry. The component failure rate is computed by multiply factors according to the current mission profile. This approach is similar to MIL-HDBK-217 [2] and Bellcore's [11]. Critical factors, such as operational cycling conditions and temperature variations are included in the mission profile. The key assumption that RDF 2000 holds is that an electronic components does never reach its wear-out stage of product life due to the fact that old products will be replaced by new ones. However, the product failure rate is determined if the component's infant mortality stage of product lifetime is in the near future. Performing the burn-in stage production process, emphasizing on the material property and the manufacturing process, provides accurate data to determine product failure rate during infant mortality stage.

These reliability data handbooks are easy to use since the reliability references for a lot of components already exist. However, the Military handbook and other standards database references assume the component failure rate is a constant over time, which results in

overlooking the thermal effects that power electronic modules undergo [13]. Additionally, the root cause of component failure is not specified and any changes in design might make the reliability reference inapplicable.

2.3. System-level Reliability Model

2.3.1. Reliability Block Diagram

System-level reliability model is a simple extension from component-level reliability model using the constant failure rate assumption from Military-Handbook. A reliability block diagram (RBD) is a main graphic application of the system-level reliability model. The RBD decomposes the system visually and clarifies the reliability interrelationship between sub-systems and components. The system reliability depends on component reliability and system configuration from reliability point of view. Depending on the system functionality dependency on component performance, the system configuration can be of series or parallel type. Series refers to a system configuration in which one component failure results into whole system failure. Meanwhile, a parallel configuration considers the design of system redundancy, which means the system is operable as long as one component is functional.

Figure 2 provides an example of a combinatorial block diagram of series and parallel configurations. The system has Subsystem A, B and C connected in a series configuration. Subsystem B is formed by Component B_1 and Component B_2 with being linked in a parallel configuration. The failure rate of Component B_1 and B_2 is λ_2; Subsystem A and Subsystem C have failure rates λ_1 and λ_3 respectively. In this case, the functionality of the system is demonstrated as Subsystem A and C function with either of B_1 or B_2 functions. Therefore, the reliability of the system *R* is given as:

$$R = (1 - \lambda_1)[1 - \lambda_2^2](1 - \lambda_3) \tag{2}$$

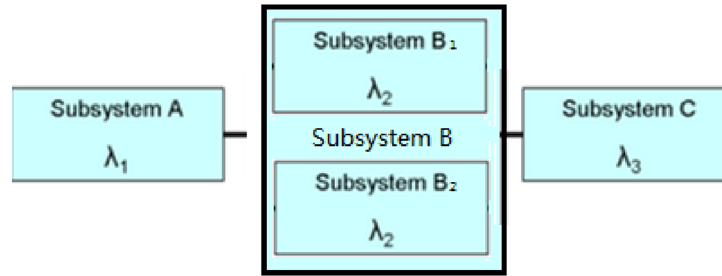

Figure 1. A reliability block diagram.

The RBD is straight forward at the product design stage. However, the priority of the failure events are not taken account in this approach. When computing system reliability, this approach assumes components fail simultaneously. Additionally, the RBD fails to capture the potential failure interaction among components. It assumes that the failure rates in the different categories are completely independent. This is, in practice, not always the case. For PEMs, the fatigue of one component can potentially trigger or accelerate the other components' failure characteristics. Therefore, RBD modeling can only be used to give a rough estimate of system reliability at early design stage.

2.3.2. Degradation Modeling

Degradation modeling is an approach using sample data and statistical distribution to analysis component/system failure characteristics. This approach is practical and suitable for any degradation process due to its simplicity. Frist, the performance degradation data are collected at each observation time shown in Table 1 [14], where x_{ij} is the degradation data of ith sample at time t_j.

Table 1. General Degradation Data Form.

Sample(i)	*Time(j)*				
	t_1	t_2	t_3	…	t_m
1	$x_{1,1}$	$x_{1,2}$	$x_{1,3}$	…	$x_{1,m}$
2	$x_{2,1}$	$x_{2,2}$	$x_{2,3}$	…	$x_{2,m}$
3	$x_{3,1}$	$x_{3,2}$	$x_{3,3}$	…	$x_{3,m}$
⋮	⋮	⋮	⋮	⋮	⋮
n	$x_{n,1}$	$x_{n,2}$	$x_{n,3}$		$x_{n,m}$

Then a distribution is selected to adequately represent the degradation behavior of the collected data as in Figure 2 [4]. In this example, normal distribution is selected. With the data at each observation time, the corresponding mean, μ_x, and standard deviation, σ_x, are estimated at each observation time. Later, the estimate value of μ_x and σ_x are fitted as a function of time as $\mu_x(t)$ and $\sigma_x(t)$. This, in general, is done using regression and least square technique.

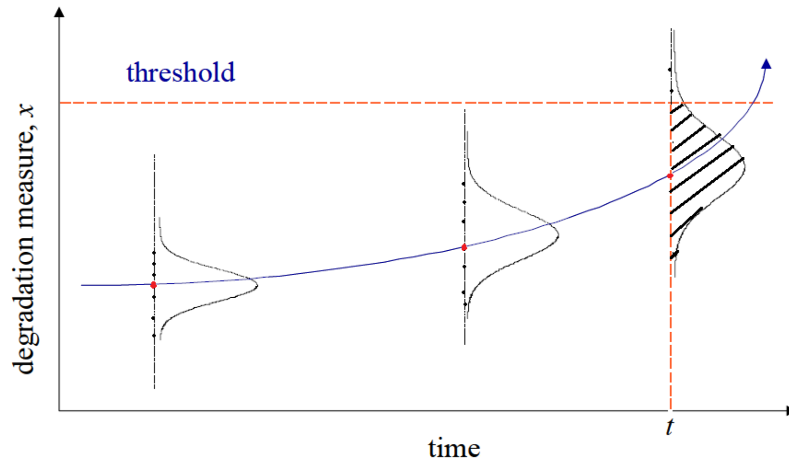

Figure 2. Degradation distribution pattern.

In the end, the component/system reliability is evaluated. In this example, the calculation is based on the assumption of normal distribution. Represented as the shaded area in Figure 2, the probability of failure, $F_H(x)$, which is the probability of the failure characteristics falls below the threshold value, is computed as:

$$F_H(x) = \int_0^H f(x, \mu_x(t), \sigma_x(t))dx \tag{3}$$

$$R_H(x) = 1 - F_H(x) \tag{4}$$

where $f(x)$ is the PDF of normal distribution for degradation process; H is the pre-defined threshold value; $F_H(x)$ and $R_H(x)$ are the cumulative probability function and the reliability function respectively.

Systems with high reliability level, like power electronic systems, the failure characteristic often are positive and gradually ascending over time. In other word, the model selected must be able to represent the dependency among the components and the positive increment in the degradation process. According to this attribute, Pan and Balakrishnan [15] propose to use gamma distribution to capture the increment of failure characteristics data based on the statistical modeling method. The correlations between these two performance characteristics is calculated with Birnbaum-Saunders distribution. With the correlation and marginal reliability distribution, the system level reliability is calculated and the component level reliability influence the system reliability is determined.

The system level modeling method seems promising in predicting system reliability. The correlation and the failure characteristics are capture at each measuring time with the degradation trend monitored. However, this method has the same problem as the RBD approach. It fails in demonstrating the main elements affecting component lifetime and the failure interaction among components. Additionally, it requires a huge sample size to obtain sufficient amount of data. If a sample fails before a measuring time, there may not be enough data available to accurately estimate the distribution parameters. Furthermore, during the estimating process, the computation errors may cause the predicted reliability to be inaccurate.

2.3.3. Competing Failure Mode and Related Derivatives

Competing failure modes methodology has been widely accepted in predicting the reliability of microelectronic devices. It classifies the failure mechanisms into hard (system

mechanical) failures and soft (system performance) failures. A hard failure is referring to the failure makes a system non-functional such as catastrophic failures. A soft failure comes from the performance degradation of the system, which is slowly losing its ability to accomplish designated functionalities to a pre-defined unaccepted level. Using a series system configuration, whichever of the failures comes first, the system fails before other failure modes appear. Modeling these two types of failures is different as well. A hard failure is normally modeled by a distribution with time-to-fail data. Meanwhile, the performance data collected over multiple time point determines the degradation distribution to modeling of a soft failure. Hard failures and soft failures can be modeled via degradation modeling approach. The system reliability is demonstrated by the combination of the hard failure distribution and the soft failure distribution.

When the hard failure and the soft failure are independent, the system reliability is the product of the hard failure relationship and the soft failure relationship. Assuming a system has *p* hard failure modes and *q* soft failure modes. For hard failure, denote the reliability of each hard failure mode as $R_{hi}(t)$, for *i*= 1,2,..., *p*. Similarly, the reliability of each soft failure mode is denoted as $R_{sj}(t)$, for *j*= 1,2,..., *q*. Together, the system reliability is calculated as:

$$R(t) = \left(\prod_{i=1}^{p} R_{hi}\,(t)\right)\left(\prod_{j=1}^{q} R_{qj}\,(t)\right) \tag{5}$$

Rafiee *et al.* [16] propose four models for dependent competing failure processes with changing degradation rate. A device is undergoing a soft failure process from degradation and shocks arriving randomly. Additionally, arriving shocks bring a hard failure process. Depending on how the degradation rate changes after shock arriving, the device reliability is defined as the product of the soft failure and the hard failure.

The competing failure mode is often used with degradation modeling. Yang and Xue [17] assume the degradation level follows a standard normal distribution when degradation process is

modeled. As the means of standard deviations of the degradation data are estimated at each time point, the functions of the mean and standard deviation are built. In this case, the reliability of product can be evaluated by the standard distribution according to the values of the mean and the standard deviation. Huang and Askin [18] propose the similar method to capture the soft and hard failures of an electronic device. Assuming degradation process follows Weibull distribution, the shape parameter, β, and the characteristic life, α, are estimated as functions of time. Thus, the reliability of the electronic device can be evaluated based on the values of β and α.

The competing failure mode classified the failure modes existing in the system into different categories and capture the failure characteristic according to their statistical behaviors. However, as an extension of RDB, competing failure mode assumes the independence relationship among failure modes or components, which fails to demonstrate the potential failure interaction among components. Therefore, competing failure mode can only be used as a complementary approach to RBD at early design stage.

2.4. Bayesian Model Averaging

When using degradation modeling to compute system reliability, there are uncertainties related to models and parameters values. The principle of Bayesian statistics uses the pre-determined prior distribution to compute posterior distribution and likelihood function of data. Based on Bayesian statistics, Bayesian model averaging is a more comprehensive approach to assess model uncertainty. For a system in which two or more competing failure mechanisms causing the system break-down, Bayesian model averaging is helpful for addressing the significant uncertainties among factors which affects the accuracy of posterior distribution for reliability analysis.

Dependent to the data set G, the posterior distribution for the quantity of interest, q, is given as [19]:

$$pr(q|G) = \sum_{k=1}^{K} pr(q|M_k, G)pr(M_k|D) \tag{6}$$

where M_1,…, M_k are the possible posterior models considered. The posterior probability of model $M_k$is

$$pr(M_k|G) = \frac{pr(q|M_j)pr(M_j)}{\sum_{j=1}^{K} pr(q|M_j)pr(M_j)} \tag{7}$$

where

$$pr(G|M_k) = \int pr(G|\theta_k, M_k)pr(\theta_k|M_k)\, d\theta_k \tag{8}$$

is the integrated likelihood of model M_k and θ_k is the vector of parameters of model M_k.

Wang and Gao [20] propose analyzing the system reliability with both insights of failure mechanisms and understandings of observed data. They use Bayesian model averaging approach to demonstrate the effect of performance degradation failures, sudden failures and the competing failure based on the interaction of these two failure modes on the total system reliability level of complex aircraft engine systems. The performance degradation is assumed follow the Gamma process. More, to capture the correlation between performance degradation failures and sudden failures in aspect of the failure mechanism, sudden failures are defined follow the Weibull distribution where the shape parameter is characterized the performance degradation. The competing failure is defined as the joint distribution of the performance degradation and sudden failure. Applying Bayesian forecast probability density function, the total system reliability of complex aircraft engine systems, which is given the reliability of performance degradation failures, sudden failures and the competing failure, is calculated with consideration of data correlation and failure mechanism.

The Bayesian average modeling provides an effective way of combining prior information with data and inferences that conditional on the data to evaluate system reliability. However, it is difficult to select a prior distribution for the assumption of unknown parameters. In practice, due to the limited knowledge, a prior distribution cannot be specified. Further, Bayesian average modeling has a high computational cost, especially when the model has a large number of parameters. In many cases, the integrals are not feasible to compute. Therefore, Bayesian average modeling does not have a wide application.

2.5. Physics of Failure Modeling

Physics-of-Failure (PoF) model is an approach that assesses component lifetime and predicts component reliability through utilizing the knowledge of product's failure mechanisms at different life-cycle loading conditions [21]. Understanding the PoF model of power electronic modules helps researchers capture the failure characteristics and performance behaviors of power electronic modules over time. Over the past decades, two major failure mechanisms of power electronic modules: wire bond lift-off and solder joint delamination, have been observed and identified. Therefore, the corresponding PoF models have been modeled and developed.

2.5.1. Wire Bond Lift-off

The IGBT break-down occurs most of the time due to wire bond lift-off. Aluminum wire bonds are soldered onto silicon chips to connect the emitter and gate pads. The sandwich structure of power electronic module consists of different types of materials. In this case, aluminum wire and silicon chips are heterogeneous materials and soldered together. When IGBTs are loaded and functioning, they undergo temperature amplitude. Due to the large coefficient of thermal expansion (CTE) difference, aluminum out expanse silicon and cracks

start to form and propagate in the wire bonds. The thermal model of the Al-Si interface heating up is shown in Figure 3 [22].

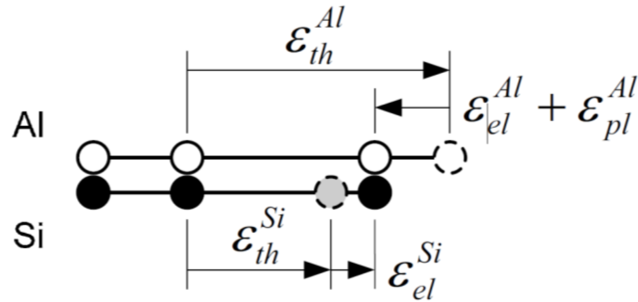

Figure 3. The thermal model of the Al-Si interface heating up.

Onuki and Koizumi [23] use transmission electron microscope (TEM) and scanning electron microscope (SEM) to investigate the microstructures of the bonding interface. Theoretically, the crack should have formed and propagated along the weakest area, which is the interconnected area of the Al-Si interface. But they found out that the crack travels along the grain boundary between the interface of Al-Si interface and Aluminum wire coincidently. Due to the small grain size the interface has, it becomes the boundaries for cracks later. This explains the reason crack doesn't propagate along the Al-Si interface.

Geohre *et al.* [22] monitor the crack propagation process in the Aluminum and Silicon interface. They found out that the crack is propagating 10-20 μm above the interface as shown in Figure 4. Ramminger *et al.*[24] study the SEM photograph of the bonding area after wire bond lifts off. The residual material of Aluminum wire is found on the pattern perimeter instead of the middle of the bonding area. It can be concluded that cracks initiate from the both end of the wire bond to the center. The mismatch of the coefficients of thermal expansion of the materials at the bonding interface leads to large plastic strains. These plastic strains drive the propagation of micro cracks leading to the fatigue failure of wire bond.

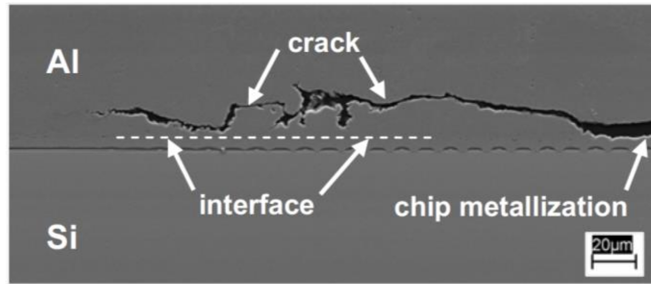

Figure 4. Crack propagates above the interface of Al-Si film.

Schafft [5] claims that smaller grains are formed, compared to Aluminum wires, in the Al-Si film by metal's re-crystallization effect during the soldering process. Therefore, grain boundaries are formed between the interface and Aluminum wires due to different grain size. According to material properties, metals with smaller grain size have greater material strength and toughness. As shown in Figure 5 [23], the bonding interface and Al-Si film have a smaller grain size compared to the wire, which indicates higher material strength in the bonding interface and Al-Si film. When thermal stress is induced, these two sections can stand the shear and tensile force better than the wire. Hence, cracks start initiating and propagating along the grain boundary.

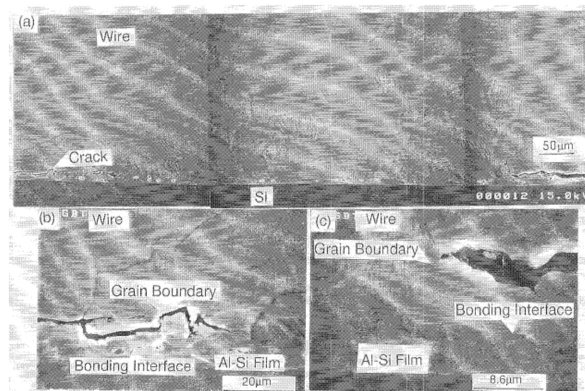

Figure 5. Wire bond interface after fatigue.

From the findings about wire bond fatigue phenomena, it can be concluded that Aluminum wire is vulnerable under the wire bond fatigue process. Therefore, PoF models have been developed to seize and describe the physical dimensional change of wire. Schafft [5]

measures the geometry change of the height of the wire loop to study the thermal fatigue induced by flexing. The model is sketched in Figure 6. The change of the height of the wire loop is given as:

$$h = h_o\left[1 + \frac{1}{8}\left(7 + \frac{3}{2}\frac{{d_0}^2}{h_o^2}\right) \times CTEw \times \Delta T\right] \tag{9}$$

where h_0 is the original height of the wire loop; CTE_w is the CTE of Aluminum wire; n represents the ratio of the wire length at the original temperature to the time that the bond is separate; d_0 is defined as the length of the wire bond span; $\Delta T$is the amplitude of temperature swing.

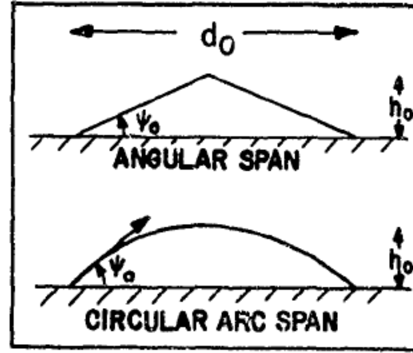

Figure 6. Geometry change of model of wire bond.

Schafft[2] also study the change of the angle of wire loop. Depending on the type of wire connections, two models have been proposed. For Angular shaped loop,

$$\cos\varphi = \cos\varphi_o\,(1 - \Delta CTE \times \Delta T) \tag{10}$$

For a circular arc shaped loop

$$\frac{\sin\varphi}{\varphi} = \frac{\sin\varphi_o}{\varphi_o}(1 - \Delta CTE \times \Delta T) \tag{11}$$

where$\varphi_o$is the original angle of the wire loop; $\Delta CTE$is the difference of CTEs between Aluminum and Silicon; ΔT is the amplitude of temperature swing.

During the thermal fatigue process, the material properties of Aluminum wire and Silicon chip change depend on the temperature amplitude. Schafft [5] monitors the main material

properties, including CTEs of Aluminum and Silicon and the elastic-plastic material law of Aluminum. Table 1 and Table 2 [5] show that the material properties of wires and silicon chip at various temperatures.

Table 2. CTEs of Wires and Chips at Various Temperatures.

	Al	Cu	Mo	Si
200K	2.15E-05	1.59E-05	4.80E-06	1.90E-06
300K	2.32E-05	1.68E-05	5.00E-06	2.50E-06
400K	2.49E-05	1.77E-05	5.20E-06	3.10E-06
500K	2.64E-05	1.83E-05	5.30E-06	3.50E-06

Table 3. Elastic-plastic Change of Aluminum at Various Temperatures.

	20°C	60°C	100°C
σ_y [MPa]	26.9597	20.6194	19.1296
ϵ_y [%]	0.29	0.37	0.38
A [MPa]	53.4067	45.1201	40.9685
B [1]	0.125738	0.126055	0.125146
ϵ_o [%]	0.4354	.20046	0.22758

Geohre *et al.*[22]estimate the plastic strains per cycle in the Al by assuming Al and Si undergo the equal strain with Si only having elastic material behavior and Al only having ideal plastic material behavior. According to Figure 3, Geohre et al. [22] model the plastic strength of Aluminum wire given as:

$$\Delta\varepsilon_{pl}^{Al} = \Delta CTE \Delta T - 2\left(\frac{\sigma_y^{Al}}{E^{Si}} + \frac{\sigma_y^{Al}}{E^{Al}}\right) \quad (12)$$

where $\Delta\varepsilon_{pl}^{Al}$is the plastic strain on Aluminum wire; $\Delta CTE$is the different of material CTE; $\Delta T$is temperature amplitude; $\sigma_y^{Al}$is the tensile force induced on the Aluminum wire by thermal fatigue process; $E^{Si}$and E^{Al} are the elastic indices for Silicon and Aluminum respectively. From the Table 2, the value of σ_y^{Al} decreases as temperature amplitude increases. Therefore, the value of $\Delta\varepsilon_{pl}^{Al}$ becomes larger as temperature amplitude increases in the equation above, which demonstrating faster fatigue failure of wire bond when temperature amplitude is high.

Another approach to test the wire bond lift-off is shear force test [5]. A horizontal force is applied by a probe to test the adhesive force of the wire bond. The degree of the bond adhesive is measured corresponding to the force which breaches the wire bond [5]. The problem of the approach is the difficulty of designing a probe that is small enough to stand the applied force and breach the wire bond. Moreover, the operator's reproducibility is also another major concern [5].

Through experiment data and measurement, Geohre et al. [22] reveal, illustrated in Figure 7, the shear force of the bonding area (sheared area) between Si chip and Al wire decreases as the bonding area (sheared area) shrinks as the degradation process deteriorates.

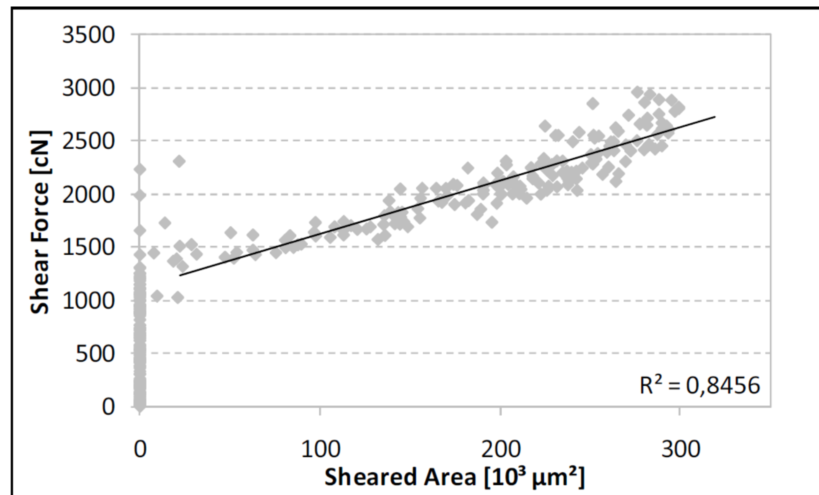

Figure 7. Shear force v.s. sheared area.

Thus, the bond degradation process can be quantified with shear force as a parameter. From Figure 7, it is clear that the shear force decreases as sheared area decreases due to crack growth and reduction of the wire bonding area [25]. The shear force at different crack length is given as:

$$F_s = \left(\frac{L-l}{L}\right) F_0 \tag{13}$$

where l is the crack length in the bonding area; L is the initial bond length; F_0 is the initial shear force existing in the wire bonding area; F_s is the remaining shear force after n cycles.

In order to capture the wire bond fatigue failure process, the component lifetime is linked to the variables contributing to component fatigue failure. Geohre *et al.* [22] measure the relationship between average shear force and number of cycles to failure in different temperature amplitude. It reveals that larger temperature amplitude results in lower number of cycles to failure. The same phenomenon is observed with average sheared area and number of cycles. It can be concluded that when crack propagates, the bonding force of Aluminum wire and Silicon chip decreases as the wire bonding area is detaching. Based on the observation, Geohre *et al.* [22] propose to use Coffin-Mason relationship to capture number of cycles to failure with the parameter of the calculated plastic strains. The equation is given as:

$$N_f = 0.309(\Delta\varepsilon_{pl}^{Al})^{-1.764} \tag{14}$$

where N_f is the number of cycles to fail and $\Delta\varepsilon_{pl}^{Al}$ is the plastic strains on wire bond.

Held *et al.*[6] report that the temperature amplitude and the median temperature are the significant factors affecting IGBT's lifetime. Taking plastic deformation and material properties into account, the model they proposed, which integrates Arrhenius approach and indicates a linear relationship.

$$N_f = A\Delta T^{\alpha} exp\left(\frac{Q}{RT_m}\right) \tag{15}$$

where ΔT is the temperature amplitude in Kelvin, A= 640, α= -5, Q= 7.8×10^4 J/mol, R is the gas constant, which is 8.314 J/(mol·K), and T_m is the median temperature in Kelvin. Taking double logarithm of the equation, this model provides a straight line relationship, shown in Figure 8, to determine the number of cycles to failure with the temperature amplitude and the median temperature as parameters.

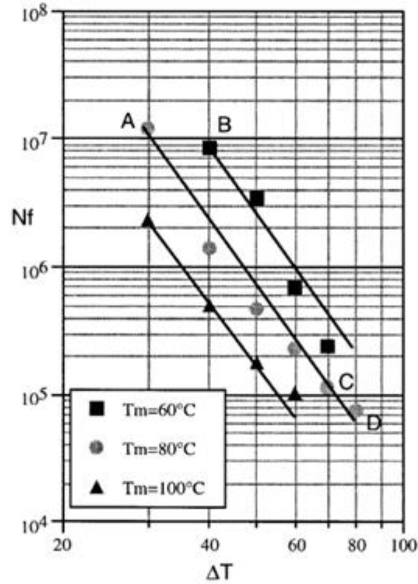

Figure 8. Number of cycles to failure v.s. ΔT and T_m.

2.5.2. Solder Joint Delamination

Solder joint is another critical component affecting IGBT system reliability. A solder joint is a component joint soldering silicon chips to the substrate and provides electrical, thermal and mechanical continuity to IGBT module. A solder joint consists with different materials depending the choices of materials, such as lead-based (SnPb) or lead-free (SnAgCu) solders. Made of different alloys, solder joint has an inhomogeneous structure [26]. Due to the thermo-mechanical stress, the grain size of solder layer grows over the elevated temperature leading to the reduction of internal energy of solder structure and the weakening of the grain boundaries [26]. Thus, voids are resulted inducing cracks propagate in solder joint. This accumulative fatigue phenomenon is illustrated in Figure 9.

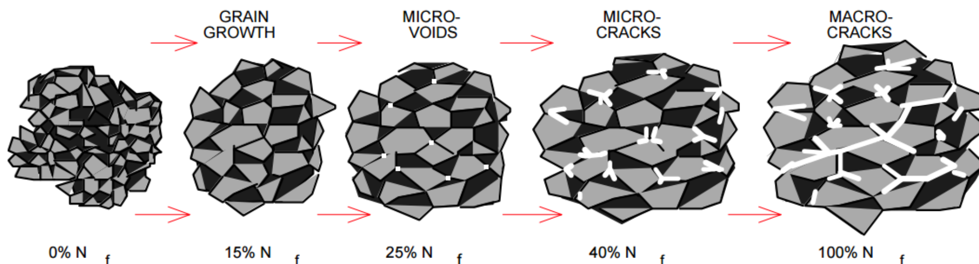

Figure 9. Accumulative fatigue phenomenon of solder joint.

To quantify the relationship between number of cycles to failure and the material damage caused by the thermal fatigue, lifetime prediction models have been developed. The most classical model is Coffin-Manson model taking into account the material damage caused by plastic strain range given the component lifetime as [27]:

$$N_f = \frac{1}{2}\left(\frac{\Delta\gamma_p}{2\varepsilon_f}\right)^{1/c} \quad (16)$$

where ε_f is the fatigue ductility coefficient and *c* is the fatigue ductility exponent depending material property; $\Delta\gamma_p$ is the plastic strain range.

On the basis of Coffin-Manson model, Solomon model [28] considers the shear plastic strain as the main cause of solder joint fatigue. The solder joint lifetime is given as:

$$\Delta\gamma_p N_f^{\alpha} = \theta \quad (17)$$

where θ is the reciprocal of fatigue ductility coefficient while α is the material constant.

The root cause of thermal-mechanical stress is temperature amplitude applied to IGBT module. Higher temperature amplitude results in strong stress in solder joint and, therefore, shorter component lifetime. Choi et al [29] use Coffin-Manson model to explain this fatigue failure process and the solder joint lifetime is given as:

$$N_f = \left(\frac{p}{\Delta T}\right)^{k} \quad (18)$$

where *p* and *k* are the material constants dependent to selected solder materials; ΔT is the temperature amplitude.

Yin et al [30] propose a strain based lifetime prediction model given as:

$$N_l = \frac{l}{q(\Delta\varepsilon_p)^g} \quad (19)$$

where *l* is the crack length solder joint; $\Delta\varepsilon_p$ is the plastic strain while N_l is the corresponding number of cycles until crack reaches the length *l*.

Mitic *et al.* [31] test the adhesion force between AlN ceramic substrates and their solder joints with a peel test. The largest decrease in the adhesion force happens after 80 thermal cycles. Hung *et al.* [32] investigate the impact of solder height on fatigue life of IGBT. The scanning acoustic microscope results indicate the solder crack length propagates from the corners of substrate towards the center as shown in Figure 10. However, the solders in high solder height show slower crack growth rate. Some thick solders show no crack found in the module after thermal cycling. Figure 7 shows the crack lengths of different solder height after 450 thermal cycles. When the solder height gets beyond 300 um, no significant crack is found. This is because increasing the thickness of solder joint restrains solder joint structure deformation [32].

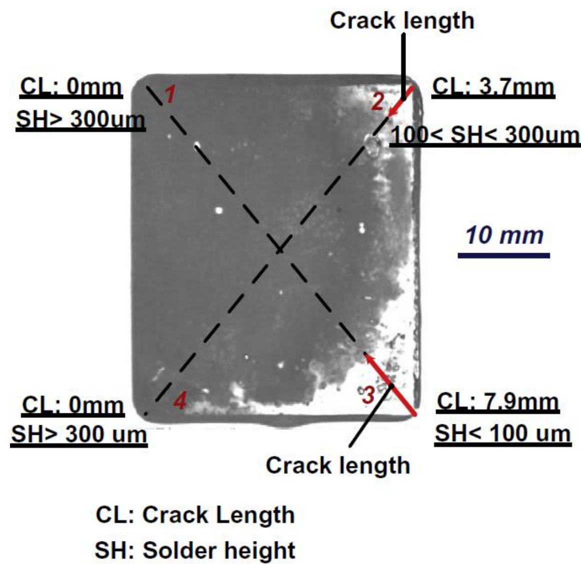

Figure 10. Crack lengths of different solder heights after 450 thermal cycles.

To quantify the impact that the physical dimension of solder joint has on component lifetime prediction, Ciappa [33] proposes an equation to capture the relationship between solder joint's number of cycles to failure and temperature swing.

$$N_f = 0.5\left(\frac{L\Delta CTE\Delta T}{\gamma x}\right)^{1/c} \tag{20}$$

where ΔCTE represents the CTE mismatch, γ and x are the ductility factor and the thickness of the solder, and L is the lateral size of the solder joint. γ and c are conservative engineering estimates dependent to materials chosen.

Recently, Advani and Yadav [8] studies the crack propagation process in solder joint. He classifies the process into two phases: crack initiation and crack propagation. Unlike the traditional approach, which monitors the change of grain size in solder alloy to determine the crack initiation, Gurmukh proposes to use the resistance of solder alloy as an indicator. Once a threshold value is reached, the solder joint is in its crack propagation phase. With Cubic Coarsening model and Coffin-Mason model proposed for each phase respectively, the all over system reliability model of solder joint is the combination of these two phases. With proper statistical assumptions for different phases, Advani and Yadav [20] evaluates the reliability model according to either the failure distribution over time or the damage accumulation on the quality characteristics.

The physics of failure model approach links the physics properties and component lifetime in depth. However, it only concentrates on one particular component's failure mechanism. Also, the correlation between components, in this case, the failure interaction between wire bond and solder joint is ignored. Additionally, the lack of probabilistic modeling makes PoF modeling fail in demonstrating the system reliability. In addition, the failure interaction between solder joint and wire bond has been studied with literature pointing out that wire bond lift-off is dominant failure mechanism. Therefore, the solder joint degradation process is triggered by wire bond lift-off phenomenon in this work.

3. PROPOSED RELIABILITY MODEL

In this section, a new system reliability model is proposed overcoming the disadvantages or research gap mentioned in literature review section. First, the proposed model uses selected PoF models to present the failure mechanism of critical components. Second, probabilistic interpretation is provided based on the PoF models. Third, system reliability is calculated in a series configuration and the failure mechanism interaction is considered. The cumulative effect of the degradation of wire bond and solder joint is updated to take account for system reliability at each cycle. Additionally, the system reliability model is classified into two phases considering the predominant of wire bond degradation process over solder joint.

3.1. Initial PoF Models Selection

The PoF models for wire bond lift-off and solder joint delamination are reviewed in the previous section. In this subsection, certain PoF models are selected to present and model the failure mechanism of wire bond or solder joint. Critical factors affecting component lifetime, such as temperature amplitude and physical dimensions, are demonstrated comprehensively in these models to provide accurate estimates on component lifetime. The selected models for wire bond and solder joint are discussed in the following sections.

3.1.1. Solder Joint PoF Model

Solder joint delamination is caused by the thermo-mechanical strain induced by the temperature amplitude. As discussed in the literature review section, the thermo-mechanical strain becomes larger when the temperature amplitude increases. Moreover, as Micol et al [7] pointed out, the initiation of solder joint failure characteristics is closely related to the geometric shape of the solder joint. Cracks propagates slower in a smaller growth rate in thick solder joint due to the deformation process is restricted [33] and the lateral size of the solder layer has a

direct impact on the magnitude of shear strain generated in solder layer. Additionally, manufactured with different alloy materials, the solder joints lifetime varies. The main categories are Pb-based solders and Pb-free solders. [34] have proven that Pb-free solders have better reliability due to high yield strength and cracks are not dependent to plastic deformation in the solder microstructure. Therefore, the model from [33] is selected to estimate the solder joint lifetime:

$$N_{fs} = 0.5\left(\frac{L\Delta CTE\Delta T}{\gamma x}\right)^{1/c} \tag{21}$$

where ΔT is the temperature amplitude of power cycling, ΔCTE is the difference of the CTEs among Solder layer materials, *x* is the thickness of the solder, and *L* is the lateral size of the solder joint; γ, which is the ductility factor, and c are conservative engineering estimates depending on materials chosen.

The reason that Equation (21) is selected is because the solder joint lifetime is predicted based on the design and operational conditions as discussed earlier. Critical physical dimensions such as thickness and lateral size of different solder materials are considered, such as *x, L, c* and γ in the equation. Thermo-mechanical strain is also captured dependent on the operational conditions, mainly temperature amplitude, ΔT. Therefore, from Equation (21), solder joint lifetime is demonstrated comprehensively.

3.1.2. Wire Bond PoF Model

The wire bond has the same cause for failure mechanism as the solder joint. The mismatch of material CTEs induces thermo-mechanical stress in wire bond when temperature amplitude is enforced. The magnitude of thermo-mechanical stress is determined by the temperature amplitude applied to the module. This relationship is often demonstrated by power law [10][22] and, therefore, temperature amplitude is the important factor account for wire bond

degradation process. Additionally, Held et al [6] test the wire bond lifetime in the same temperature amplitude but with different mean temperatures. A parallel shift is observed for different mean temperatures when the degradation data is plotted in Arrhenius model [6]. Therefore, based on these findings, the wire bond lifetime model is given as:

$$N_{fw} = A\Delta T^{\alpha} exp \frac{Q}{RT_m} \tag{22}$$

where ΔT is the temperature amplitude in Kelvin, A= 640, α= -5, Q= 7.8×10^4 J/mol, R is the gas constant, which is 8.314 J/(mol·K), and T_m is the median temperature in Kelvin.

Compared to most of the PoF models in other literatures [22][35][36], which mainly focus on the relationship between shear strain and numbers of cycles, Equation (22) details the wire bond lifetime not only with the effect from temperature amplitude, but also the parallel shift of wire bond lifetime trend from different mean temperatures due to various operational conditions as found in [6]. Therefore, the solder joint lifetime is represented comprehensively via Equation (22).

3.2. Probabilistic Modeling

From Equation (21) and (22), the number of cycles to failure for solder joint and wire bond can be easily estimated. However, in practice, the fatigue damage is of stochastic nature due to the randomness in material fatigue behavior and loading conditions [37]. In order to provide more realistic estimate of system reliability, it is, therefore, necessary to convert deterministic modeling into probabilistic modeling. The following sections provide detailed discussion on probabilistic modeling.

First, component lifetime is closely related to temperature amplitude applied to PEM modules. Higher temperature amplitude results in shorter component lifetime. Treating temperature amplitude as the stress, it is reasonable to use the S-N curve to demonstrate the

relationship between component lifetime and temperature amplitude. The probabilistic interpretation for the relationship of temperature amplitude and number of cycles to failure is illustrated in Figure 11. In Figure 11, the component lifetime is depicted and the numbers of cycles to failure at different temperature amplitudes are shown. The estimate component lifetime decreases as temperature amplitude increases, i.e. $\Delta T_1 \geqslant \Delta T_2 \geqslant \Delta T_3$.

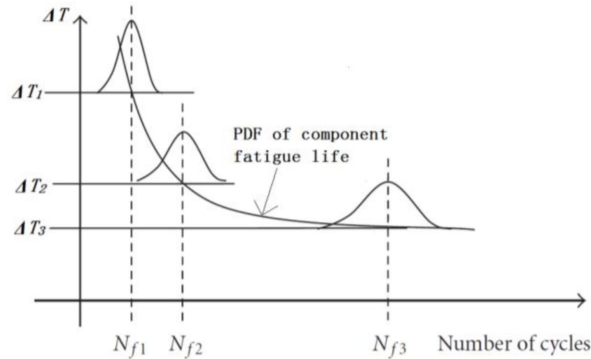

Figure 11. Probabilistic interpretation between ΔT and N_f.

Second, to capture the stochastic behavior of lifetime data, a statistical distribution is selected. Rathod et al [37] pointed out that the fatigue lifetime shows stochastic behavior of a certain distribution even under constant stress level. Literature highlights that fatigue life data follows normal or lognormal distribution under constant or random loading of stress [38] [39] [40]. Therefore, to estimate the expected component lifetime and its variation at any given cycle, normal distribution is used for both failure models as:

$$L_s \sim norm\{\mu_s, \sigma_s^2\} \tag{23}$$

$$L_w \sim norm\{\mu_w, \sigma_w^2\} \tag{24}$$

where N_s is normal distribution for solder joint lifetime data, μ_s and σ_s^2 represent the corresponding mean and variance for solder joint lifetime distribution respectively. Similarly, N_w is normal distribution for wire bond lifetime data, μ_w and σ_w^2 represent the corresponding mean and variance for wire bond lifetime distribution respectively.

Additionally, components tend to fail in a short time span if the applied stress level, *ΔT*, is high. The phenomena is observed as the spread of the distribution increases as component lifetime increases and temperature amplitude decreases. Therefore, it is reasonable to assume the variance is proportion to the estimate lifetime. From the above rationale, the probability density function of component lifetime for both models at any specific cycle, *N,* are given as:

$$f_w(N) = \frac{1}{\sigma_{N_{fw}}\sqrt{2\pi}} exp\left(-\frac{1}{2}\left(\frac{N-N_{fw}}{\sigma_{N_{fw}}}\right)^2\right) = \frac{1}{\sigma_{N_{fw}}\sqrt{2\pi}} exp\left(-\frac{1}{2}\left(\frac{N-N_{fw}}{m_w \times N_{fw}}\right)^2\right) \qquad (25)$$

$$f_s(N) = \frac{1}{\sigma_{N_{fs}}\sqrt{2\pi}} exp\left(-\frac{1}{2}\left(\frac{N-N_{fs}}{\sigma_{N_{fs}}}\right)^2\right) = \frac{1}{\sigma_{N_{fs}}\sqrt{2\pi}} exp\left(-\frac{1}{2}\left(\frac{N-N_{fs}}{m_s \times N_{fs}}\right)^2\right) \qquad (26)$$

where m_w and m_s the proportion coefficients for wire bond and solder joints.

3.3. Modeling Component Failure Mechanism Interaction

In the previous section, PDF of fatigue life for each component is defined and established. However, to provide more realistic estimate to model system reliability, the lifetime model needs to take account for the failure mechanism interaction between wire bond and solder joint degradation process. In this particular work, the increase in junction temperature caused by initiation of one failure or degradation process and its impact of other degradation processes have been investigated.

For wire bond lifting off phenomenon, one wire lifting off the bonding area will cause increases in the current load on the remaining wires. This phenomenon worsens the self-heating in the remaining wires and causes higher junction temperature in bonding area. The changes in junction temperature induced by the degradation process of wire bond with different bonding techniques is shown in Figure 12 [41].

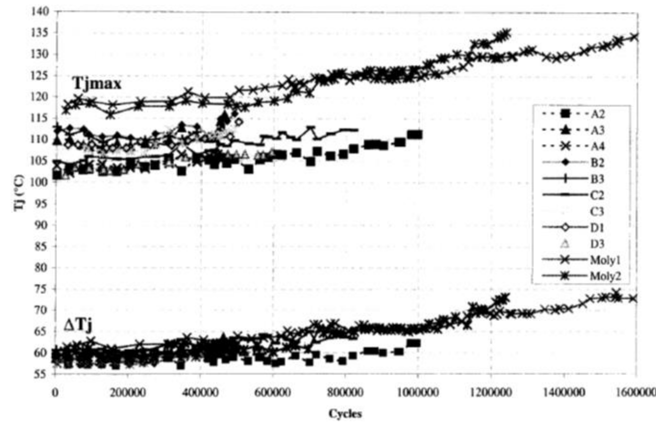

Figure 12. Junction temperature values versus the number of cycles.

The wire bond lift-off is accelerated due to the increased junction temperature. Cracks propagate towards the center of the bond foot until the wire completely lifts off from the bonding area causing the termination of the mechanical and electrical contact of the metallization.

Moreover, increase in junction temperature results in increase in collector-emitter voltage (V_{CE}) [42] and, therefore, V_{CE} is used as an indicator for wire lifting. Gradual increase in V_{CE} has been detected, shown in Figure 13, regardless to wire bonding techniques during power cycling process [41]. Additionally, the literature shows majority of the tested modules failed due to wire bond lift-off phenomenon [47]. From the above observation, it is concluded that wire bond lift-off is the predominant failure mechanism for IGBT modules when temperature amplitude is under 130 K [34] [42] [44].

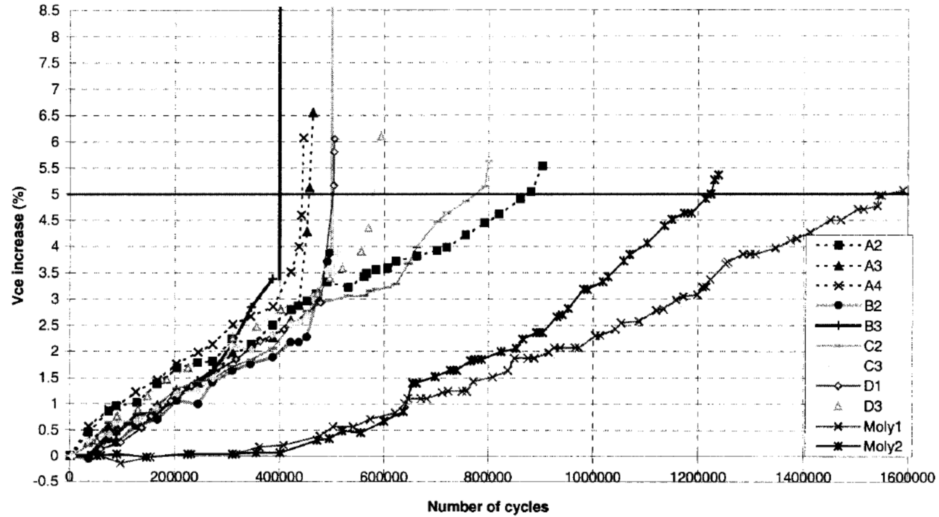

Figure 13. V_{CE} increases versus the number of cycles.

Similar to wire bond, the solder fatigue phenomenon occurs in the degradation process due to the thermo-mechanical stress. The main failure phenomenon due to thermo-mechanical stress causes solder delamination with voids created between chip and chip solder layer. The formation of these voids impedes heat dissipation since heat has to go around the voids to dissipate [33]. This impediment in heat dissipation results in further increase in junction temperature. The solder layer delamination also causes the increase in the thermal resistance in solder joint. It is found that the increasing thermal resistance is often followed by the changes in the voltage of gate-emitter (V_{GE}). Thus, it is reasonable to monitor the solder layer delamination with the change in V_{GE}. The relative change of the V_{GE} at lead-free solder joints at various temperature amplitudes is measured and shown in Figure 14. The relative change of V_{GE} increases sharply when temperature amplitude is set at 110K. However, it does not show any signs of change on V_{GE} when the junction temperature is 60K.

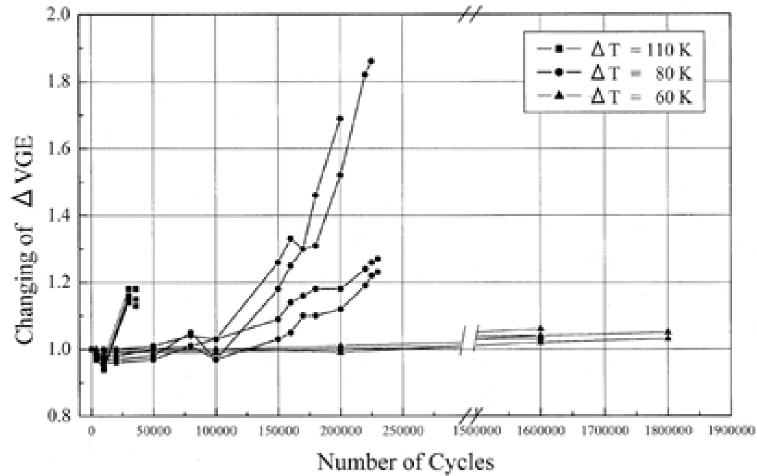

Figure 14. Relative change of V_{GE} versus the number of cycles.

Based on the observation above and combined with the wire bond failure process, the behavior of solder joint degradation is further detailed according to the change of V_{GE} depicted in Figure 15. The relative change of V_{GE} remains constant at the beginning of the power cycling test since no sign of solder degradation shown. However, as wire bond lift-off is the predominant failure mechanism, junction temperature rises slowly due to the self-heating phenomenon of wires as the wire bond fatigue continues. When junction temperature increases to a certain magnitude, cracks are initiated in solder joint causing changes in V_{GE}. As illustrated in Figure 15, the crack initiation phase ends at N_{SI} cycles and crack propagation phase starts. Therefore, the change in V_{GE} value can be used as a measure to decide when solder joint degradation is triggered. The subsequent increase in junction temperature can be attributed to the cumulative effect of the degradation process of wire bond and solder joint.

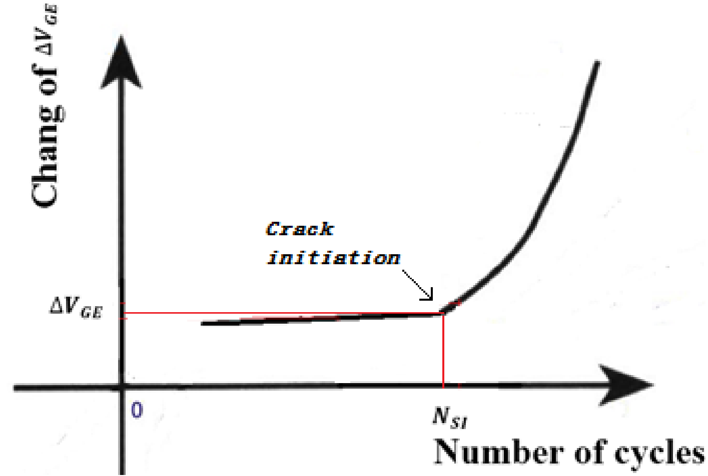

Figure 15. Change of ΔV_{GE} in solder joint.

From the reasoning above, the junction temperature increases at faster rate once the degradation of solder joint starts. Simultaneously, the degradation process of solder joint and wire bond is accelerated by the increasing junction temperature. Therefore, the failure interaction between wire bond and solder joint occurs through the increasing junction temperature. Therefore, capturing the increasing junction temperature becomes the focal point of this work to model failure interaction and provide realistic system reliability prediction. This process is detailed as follows.

Considering only wire bond and solder joint IGBT subjected to degradation process and the predominance of wire bond degradation process over solder joint, it is reasonable to consider that failure mechanism of wire bond starts first in most of cases. Therefore, the initial increase in junction temperature is resulted from the wire bond failure process. The junction temperature is given as:

$$\Delta T' = \Delta T + \Delta T_{jw} \tag{27}$$

where ΔT is original temperature amplitude and ΔT_{jw} is the amount of increase in junction temperature caused by wire bond.

Once the cracks start at N_{SI}th cycle, crack propagation leads to solder joint fatigue and junction temperature is raised resulting from the cumulative effect of both wire bond and solder joint fatigue. Therefore, the increase in junction temperature after N_{SI}th cycle is given as:

$$\Delta T' = \Delta T + \Delta T_{js} + \Delta T_{jw} \tag{28}$$

where ΔT is original temperature amplitude; ΔT_{jw} is the amount of increase in junction temperature caused by wire bond while ΔT_{js} is the amount of increase in junction temperature caused by solder joint.

The heat generated by the rising junction temperature due to component degradation can be determined via Joule's Law with component failure indicators. For the purpose of simplicity, we assume that there is no heat loss. According to First Law of Thermodynamics, the heat generated by the rising junction temperature by wire bond or solder joint can be given as:

$$\Delta Q_s = \frac{\Delta V_{GE}{}^2 N}{I} = C_s m_s \Delta T_{js} \tag{29}$$

$$\Delta Q_w = \frac{\Delta V_{CE}{}^2 N}{I} = C_w m_w \Delta T_{jw} \tag{30}$$

where N is the number of cycles; I is the current applied on the module; C_s and C_w are the specific heat capacity of component solder joint and wire bond; m_s and m_w are the mass of solder joint and wire bond; ΔT_{js} and ΔT_{jw} are the amount of the temperature raised by solder joint and wire bond respectively.

Thus, the rising junction temperature induced by the degradation process of solder joint and wire bond at any given cycle are given as:

$$\Delta T_{js} = \frac{\Delta V_{GE}{}^2 N}{I C_s m_s} \tag{31}$$

$$\Delta T_{jw} = \frac{\Delta V_{CE}^2 N}{IC_w m_w} \quad (32)$$

To obtain the value of V_{GE} and V_{CE} at the corresponding cycle, the statistical behavior of V_{GE} and V_{CE} is studied. From Figure 14 and Figure 15, V_{GE} and V_{CE} monotonically increase as the power cycling continues. Through the result of empirical degradation model, the failure characteristics of degradation process grows exponentially as a function of time and therefore, exponential distribution provides a good fit to capture the behavior of the increased thermal resistance as shown in Figure 16 [45]. Therefore, it is reasonable to model the behavior of V_{GE} and V_{CE} with exponential fit.

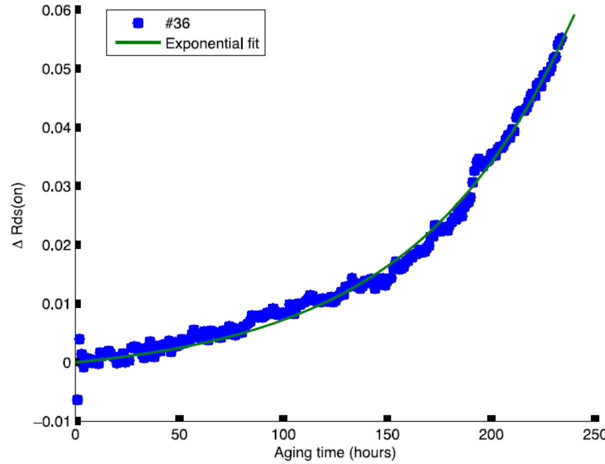

Figure 16. Behavior of thermal resistance.

With the increased junction temperature being calculated through Equation (31) and (32) at any given cycle, the effect of failure mechanism interaction is incorporated with the expected lifetime of wire bond and solder joint modified. The modified equations for the expected lifetime of solder joint and wire bond are given as:

$$N_{fs}^{'} = 0.5(\frac{L\Delta CTE\Delta T'}{\gamma x})^{1/c} \quad (32)$$

$$N_{fw}^{'} = A\Delta T'^{\alpha} exp\left(\frac{Q}{RT_m}\right) \quad (33)$$

where $N_{fs}^{'}$and $N_{fw}^{'}$ are the number of cycles to failure for solder joint and wire bond respectively with the updated junction temperature; the rest of the remaining terms are the same as defined in Equation (21)(22).

The probabilistic model is updated with the increase junction temperature is given as:

$$L'_s(N) \sim n\{\mu'_s(N), \sigma'^2_s(N)\} \tag{35}$$

$$L'_w(N) \sim n\{\mu'_w(N), \sigma'^2_w(N)\} \tag{36}$$

3.4. System Reliability Modeling

The system reliability is computed based on a series configuration since either of wire bond or solder joint fails will results in the break-down of IGBT module. In general, the system reliability for series configuration is calculated as the product of the reliability of each individual component as given below:

$$R(N) = R_1(N) \times R_2(N) \times \cdots \times R_k(N) \tag{37}$$

where k is the total number of components in system.

In this work, only wire bond and solder joint are considered as critical failure mechanisms causing the degradation process of IGBT module. Therefore, Equation (37) is modified as:

$$R(N) = R'_s(N) \times R'_w(N) \tag{38}$$

where $R_s(N)$ is the reliability of solder joint at *N*th cycle and $R_w(N)$ is the reliability of wire bond.

However, reliability prediction for IGBT module based on Equation (38) is not realistic because it assumes independence relationship between solder joint and wire bond and ignore the interaction among failure mechanisms. The failure mechanism interaction is demonstrated as one component's fatigue failure can trigger or accelerate other component's failure mechanism

through increased junction temperature. Therefore, to demonstrate the effect of failure mechanism interaction, system reliability is computed in two phases according to Section 3.3.

In the first phase, before N_{SI}th cycle, wire bond lift-off is the predominant failure mechanism in IGBT module because solder joint does not show any sign of degradation. Thus, the product lifetime is solely depending on the performance of wire bond. The increases in junction temperature is attributed to the fatigue failure of wire bond lift-off and the failure characteristics is affected by the updated junction temperature at any given cycle.

At each cycle *N*, the increases in junction temperature attributed by degradation process of wire bond can be computed through Equation (29) and the overall junction temperature is given by Equation (27). With the overall junction temperature, the estimate component lifetime is computed via Equation (34) and the probabilistic distribution of wire bond lifetime is updated. Therefore, the system reliability is the probability that the IGBT module can survives beyond the expected lifetime cycle of wire bond at the current cycle:

$$R_{system} = R'_w(N > N'_w) \tag{39}$$

Second phase, starting from N_{SI}th cycle, due to the increased junction temperature induced by wire bond degradation, solder joint degradation process is triggered and accelerated. Meanwhile, solder joint degradation process affects junction temperature and accelerates the propagation of crack in wire bond failure process. Thus, the degradation process of both components are accelerated and system reliability is reduced tremendously.

Similarly to the first phase, the increase junction temperature caused by degradation process of wire and solder joint is captured by Equation (29) and (30). Thereafter, overall junction temperature can be computed via Equation (28). The probabilistic distribution for wire bond and solder joint is updated once the overall junction temperature is obtained. Therefore, the

system reliability is the product of the probability that the IGBT module can survives beyond the expected lifetime cycle of each component at the current cycle:

$$R_{system} = R'_w(N > N'_w) \times R'_s(N > N'_s) \tag{40}$$

Therefore, dependent to the above reasoning, the system reliability is computed in two situations and the N_{SI}th cycle is the critical value for the prediction process. The combine model is provided as follows.

$$\Delta T' = \begin{cases} R'_W(N > N'_w) & for \quad N < N_{SI} \\ R'_w(N > N'_w) \times R'_s(N > N'_s) & for \quad N \geq N_{SI} \end{cases} \tag{41}$$

4. EXAMPLE

In this section, a numerical example is provided to demonstrate the applicability and effectiveness of the proposed reliability approach.

4.1. Background

An IGBT module has an inhomogeneous structure consisting of different components with various CTEs. The free expansion of component materials is restricted as they are bonded together. The temperature amplitude IGBT module undergoes while functioning leads to the degradation of the module. Due to the larger mismatch of CTEs, thermo-mechanical stress is generated and occurs in the solder joint and wire bonding area when the temperature amplitude induces. Since interconnected, the restriction or limitations on the thermal expansion of material leads to initiation of cracks causing degradation in solder joint and wire bonding area. The mechanical and electrical connections among components are terminated once cracks slowly propagate to a critical length separating the component from the module in wire bonding area and solder joint layer and marking the failure of the module.

As evident from Equation (21) and (22), the expected lifetime of component wire bond and solder joint can be estimated once the temperature range of power cycling and the physical dimensions of components are decided. However, due to the interaction among failure mechanisms during the degradation process, the component expected lifetime gets reduced. The example is based on the failure behavior of IGBT module during power cycling. Solder joint and wire bond go through a thermal fatigue process accompanied with cracks initiated and propagate in these components. As mentioned in previous section, the inspection for the failure behaviors of solder joint and wire bonding area can be executed by monitoring the increase pattern of V_{GE} and V_{CE} due to the proportional relationship between the pattern and the failure behavior. Once

the increase pattern of V_{GE} and V_{CE} is captured, the overall junction temperature can be computed for further reliability analysis. The system reliability is demonstrated considering the predominance of wire bond lift-off and the comparison to the independence assumption among components.

4.2. Data Collection

In this work, it is assumed that the degradation process of IGBT module is caused by power cycling. The data needed for the proposed reliability method are cited from literature [6] [22] [34]. The IGBT specimen is made up with wires bonded onto a silicon chip. Solder joints are used as medium to connect the silicon chip, substrate and water cooler. The experiment is set up in an ambient that the temperature amplitude and the medium temperature are preset, which is achieved via stable current applied to the specimen and water cooler frequently functioning [6] [22] [34]. The electrical power load is applied to the IGBT chip in the module and the conducting is 2 seconds for each cycle [6]. The accuracy of the temperature amplitude is verified with the application of temperature sensors as well [6]. The change of component failure characteristics is monitored during the power cycling test especially the value of V_{CE} [6] and V_{GE} [22]. With all the data found from literature, the statistical behavior of component degradation process is studied and foundation of the data analysis is built. This allows the proceeding of the Data Development stage and the advancement of the proposed reliability model.

4.3. Data Development

4.3.1. Component Material Parameters

To accurately predict system reliability, the appropriate data were collected carefully from the existing literature that focus on lifetime estimate and reliability analysis of solder joint

and wire bond. To ensure required data type for our proposed model, the data development plan is discussed in the following sections.

In order to estimate the expected component lifetime, temperature amplitude and the temperature range need to be predefined according to the selected PoF models for wire bond and solder joint. A pre-set temperature amplitude is produced as $\Delta T= 80K$ ranged from 20°C to 100°C. For solder joint lifetime, the information of physical dimension and composited materials is further needed. For wire bonding area, the chip is connected with aluminum wire with a content of 99% or more. The diameter of the wires is 400 μm [22]. Tin-silver-based alloy containing no lead is used as the solder joint material [34] to solder the silicon chip and substrate.

With the component materials selected for wire bond and solder joint, the corresponding parameters for material property are listed below in Table 4.

Table 4. Component Parameters Summary.

Parameters	Values	Sources
Al density(Kg/m3)	2689	[46]
Solder density(kg/m3)	7370	[46]
Al specify (JKg-1C-1)	951	[46]
Solder specify (JKg-1C-1)	150	[46]
Al CTE(ppm/°C)	24	[46]
Silicon CTE(ppm/°C)	3.2	[46]
Solder joint CTE(ppm/°C)	23	[46]
Wire bond pad size(m)	0.004	[6]
Wire thickness(m)	0.004	[22]
Wire bond length (m)	0.004×2.5	[47]
Chip solder pad size(mm)	6.95×6.45	[48]
Chip solder height(mm)	0.1	[6]
Current(A)	300	[6]

4.3.2. V_{CE} and V_{GE} Measurement

Using degradation data available from literature [6] [22], the regression models of V_{CE} and V_{GE} are developed in the next two subsections.

1) The change in the value of V_{CE} is used as an indicator of wire bond fatigue failure. This is due to the fact that V_{CE} changes in accordance with the change of junction temperature, which resulted from the fatigue failure of wire [6].

   V_{CE} is normally measured via either online or static measurement method. For online measurement, the change of V_{CE} is measured when power cycling is running; while static measurement interrupts power cycling periodically for V_{CE} measurement. Static measurement is preferred in most cases due to the convenience of comparing test results under various conditions [6]. Figure 17 displays the measurement of V_{CE} and the increasing pattern is captured with regression techniques with number of cycles, *N*, as the parameter. The model is fitted as:

$$V_{CE} = 3129.7 \times e^{4\times10^{-5}N} \tag{42}$$

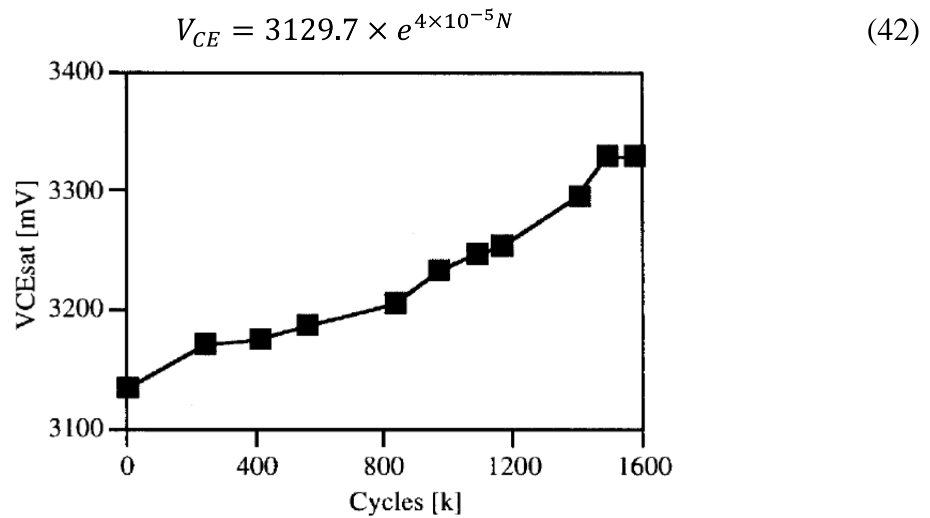

Figure 17. V_{CE} value versus number of cycles.

2) As pointed out earlier, the solder joint fatigue failure affects the change of V_{GE}. Similar to V_{CE}, static measurement is used to record the value of V_{CE} at specific cycles. The data of V_{GE} is obtain via Figure 15 from [42]. Based on the data in Figure 15, regression model is fitted and the regression models for V_{GE} is:

$$V_{GE} = 3975.4 \times e^{0.0026\times10^{-5}N} \tag{43}$$

4.4. Data Processing and Reliability Analysis

With the parameters listed in Table 1, the expected lifetime for wire bond and solder joint is calculated through Equation (21) and (22). Since the temperature amplitude is preset as ranged from 20°C to 100°C, the mean temperature amplitude, $\Delta T_m = \frac{20+100}{2} = 60℃$. Therefore, the expected component lifetime for solder joint and wire bond is computed respectively as:

$$N_{fs} = 0.5 \times \left(\frac{0.0004\times(21.5-3.2)\times 80}{1.1\times 0.0004}\right)^{\frac{1}{-0.49}} = 338.78\, K\ cycles \quad (44)$$

$$N_{fw} = 640 \times 80^{-5} \times exp\left(\frac{7.8\times 10^4}{8.314\times(273+60)}\right) = 355.98\, K\ cycles \quad (45)$$

The cycle that causes 3% increase in V_{GE} is treated as N_{SI}th cycle in which the solder joint shows the sign of fatigue. In other words, the crack starts to initiate and propagate in solder joint caused by high junction temperature. Using this criterion and Equation (40), N_{SI}th cycle is calculated as:

$$N_{SI} = \frac{\ln\frac{(1+3\%)\times 3129.7}{3129.7}}{4\times 10^{-5}} = 54.745\, K \quad (46)$$

Based upon the calculation above, *54.745K*th cycle is the cycle that the solder joint is considered to start fatiguing and taken into account for system reliability prediction. Hence, from this point on, junction temperature is effect by not only the degradation process of wire bond, but also solder joint. According to this finding, the increase junction temperature is calculated as the following equation depending to the specific cycle

$$\Delta T' = \begin{cases} \Delta T + \Delta T_{jw} & for \quad N < 54.745 \\ \Delta T + \Delta T_{jw} + \Delta T_{js} & for \quad N \geq 54.745 \end{cases} \quad (47)$$

Using the parameters from Table 3 via Equations (31) and (32) defined in proposal model, the change in junction temperature due to component degradation is computed as a function of cycles:

$$\Delta T_{jw} = \frac{\Delta V_{CE}^2 N}{IC_w \rho_w v_w} = \frac{3129.7 \times e^{4\times10^{-5}N} \times N}{300\times951\times2869\times0.004\times2.5\times0.004} = 0.956 \times e^{4\times10^{-5}N} \times N \quad (48)$$

$$\Delta T_{js} = \frac{\Delta V_{GE}{}^2 N}{IC_s \rho_s v_s} = \frac{3975.4 \times e^{0.0026\times10^{-5}N} \times N}{300\times7370\times150\times0.00695*0.00645\times0.001} = 267.37 \times e^{0.0026\times10^{-5}N} \times N \quad (49)$$

Therefore, the overall updated junction temperature is calculated using Equation (16) as shown in Figure 18.

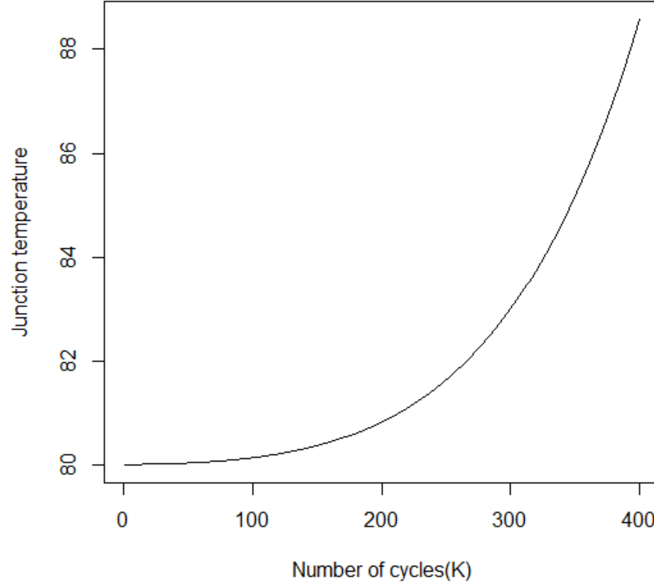

Figure 18. Increasing pattern of junction temperature during power cycling.

Based on observation from Figure 18, the junction temperature increase reveals the impact of component degradation process on junction temperature as demonstrated by the slope of the curve increase over the number of cycles. Clear increase on the curve is observed as power cycling continues, which indicates the further component degradation process due to increase in the junction temperature.

With the overall junction temperature updated at each cycle, the expected component lifetime is calculated as:

$$N_{fs}^{'} = 0.5\left(\frac{L\Delta CTE\Delta T'}{\gamma x}\right)^{1/c} \quad (50)$$

$$N_{fw}^{'} = A\Delta T'^{\alpha} exp\left(\frac{Q}{RT_m}\right) \quad (51)$$

The lifetime data for both components are assumed to follow normal distribution since normal distribution provides good fit to estimate the number of cycle to fail on component that under constant or random amplitude loading conditions [37]-[40]. It is testified by plotting fatigue life distributions in different probability papers and examining the goodness-of-fits of these distributions with chi-square techniques [46]. For the purpose of simplicity, a fix proportion 30% of the expected life is considered for the variance for both components. Hence, the probabilistic model is updated with the increase junction temperature is given as:

$$R'_s(N) \sim norm\{\mu'_s(N), 30\%\mu'^2_s(N)\} \tag{52}$$

$$R'_w(N) \sim norm\{\mu'_w(N), 30\%\mu'^2_w(N)\} \tag{53}$$

Based on Equations (39) and (40), the component reliability and system reliability are calculated at every specific cycle. For example, in pth cycle, if p is less than N_{SI}, the system reliability is only dependent to the wire bond degradation process. Hence, the increase junction temperature due to it is calculated as:

$$T_{jwp} = 0.956 \times e^{4\times10^{-5}N_p} \times N_p \tag{54}$$

The overall junction temperature is computed as:

$$\Delta T_p{}' = \Delta T_j + \Delta T_{jwp} = \Delta T + 0.956 \times e^{4\times10^{-5}N_p} \times N_p \tag{55}$$

With the updated component lifetime on wire bond computed with Equation (10) as:

$$N'_{fwp} = A\Delta T_p{}'^{\alpha} exp\left(\frac{Q}{RT_m}\right) \tag{56}$$

the system reliability of IGBT module, according to Equation (13), is computed as:

$$R_{system} = R'_w(N > N'_w) = norm\left(N_p > N'_{fwp}\right) \tag{57}$$

However, if p is greater than N_{SI}, the system reliability is not only dependent to the wire bond degradation process, but also relies on the solder joint lifetime. Hence, the increase junction temperature due to both components is calculated respectively as:

$$T_{jwp} = 0.956 \times e^{4\times10^{-5}N_p} \times N_p \tag{58}$$

$$\Delta T_{js} = 267.37 \times e^{0.0026\times10^{-5}N_p} \times N_p \tag{59}$$

The overall junction temperature is computed as:

$$\begin{aligned} \Delta T_p' &= \Delta T_j + \Delta T_{jwp} + \Delta T_{js} \\ &= \Delta T + 0.956 \times e^{4\times10^{-5}N_p} \times N_p + 267.37 \times e^{0.0026\times10^{-5}N_p} \times N_p \end{aligned} \tag{60}$$

With the updated component lifetime on wire bond and solder joint computed with Equation (33) (34) as:

$$N_{fwp}^{'} = A\Delta T_p{}'^{\alpha} exp\left(\frac{Q}{RT_m}\right) \tag{61}$$

$$N_{fsp}^{'} = 0.5\left(\frac{L\Delta CTE\Delta T_p{}'}{\gamma x}\right)^{1/c} \tag{62}$$

the system reliability of IGBT module, according to Equation (38), is computed as:

$$\begin{aligned} R_{system} &= R'_w(N > N_w') \times R'_s(N > N_s') \\ &= norm\left(N_p > N_{fwp}'\right) \times norm\left(N_s > N_{fsp}'\right) \end{aligned} \tag{63}$$

With this computing algorithm, the system reliability and the component reliability are computed at each cycle. The result is plotted in Figure 19. For the purpose of comparison, the system reliability with independent assumption, which does not consider failure mechanism interaction between crticial components, is also plotted in Figure 19.

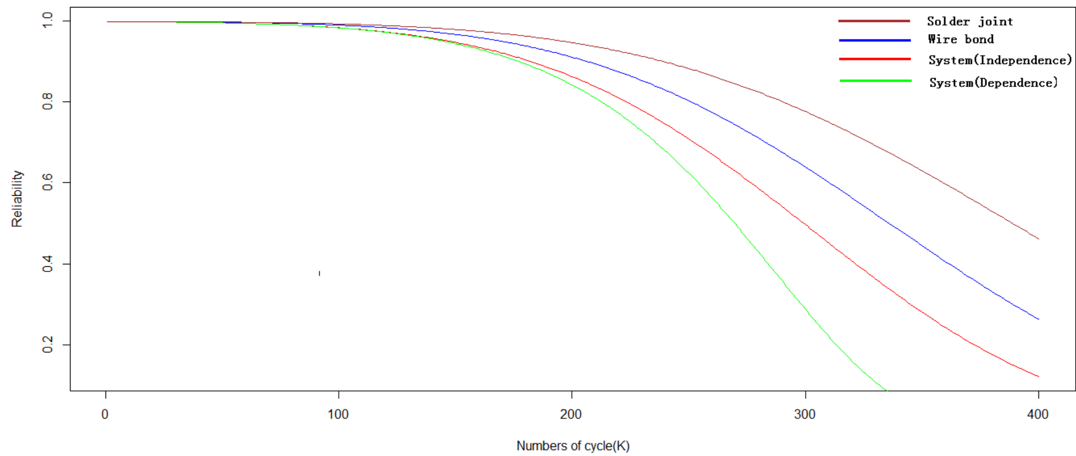

Figure 19. Component reliability and system reliability.

In Figure 19, the system reliability with independent assumption and the system reliability are represented in the red curve and the green curve respectively. Meanwhile, the component reliability curves of wire bond and solder joint are marked in blue and brown accordingly. All curves have a decreasing pattern as the numbers of cycles continue. Early junction temperature increases is negligible and do not effect product lifetime since no sign of obvious fatigue is observed from Figure 19. As power cycling continues, the wire bond starts to fatigue as the blue curve declines after 150K cycles. Due to the increase junction temperature and the failure mechanism interaction, the solder joint degradation process follows at 200K cycles and both components' degradation rates gradually rise especially after 250K cycles. The wire bond reliability curve is under the solder joint reliability curve during this power cycling test, meaning that the wire bond maintains its predominant failure mechanism and influences the system reliability the most since it fails faster. This confirms the observation of the predominance of wire bond failure mechanism when temperature amplitude is under 130K in [34] [42] [44]. In such a case, reliability improvement on wire bonding area is critical and can result in late initiation of wire bond degradation process, which potentially alleviate the mutual

effect of failure interaction and postpones the solder joint degradation. Therefore, the system lifetime is enhanced and reliability is improved.

The system reliability with dependence and independence assumption are computed and plotted in Figure 19 as well. At the beginning of power cycling, the green curve and the red curve overlap with each other meaning there is no reliability prediction difference given only the wire bond degradation process is involved. However, as power cycling continues, huge discrepancy emerges. This phenomenon is noted when the solder joint degradation process pitches in. From 190K cycles, at which solder joint starts to show recognizable drop on its reliability curves, the distinct gap between the red curve and the green curve is observed indicating the system is failing faster than it is predicted with the dependent assumption. With the consideration of failure interaction, the green curve clearly shows that system degrades faster than the red curve, meaning the proposed reliability method is able capture the interaction between these two components' failure mechanisms which the independent assumption fails to. The effectiveness and accuracy of the proposed reliability method is amplified after 250K cycle, at which the system is functioning in its most vulnerable state and the mutual effect of component failure mechanisms interaction is magnified due to the rapid increase in junction temperature. In Figure 18, junction temperature increases at faster rate after $250K$ cycles. Meanwhile, in accordance, a sharp drop on system reliability after $250K$ cycles on the green curve can be observed in Figure 19. Based upon this phenomenon, the significant influences of the failure mechanism interaction and junction temperature on system reliability is demonstrated. However, a smoother decreasing trend is shown on the red curve. Due to the assumption of independence relationship between components, the potential component failure mechanism interaction is not considered, which leads to invalid interpretation on system reliability especially

in the late stage of product life. Furthermore, the independence assumption computes the system reliability as the product of the component reliabilities as a series configuration, the computing result tends to emphasizes on the importance of the component that contributes a higher portion in the calculation. In our case, it is the wire bond due to its predominant failure mechanism. Reflected in Figure 19, the red curve is almost parallel to the blue curve after 290K cycles. The reasoning above demonstrates the effectiveness and validity of the proposed reliability model and the rationale of considering failure interaction to provide more realistic estimates of system reliability. At the same time, reliability computation with the independence assumption might overestimate the system reliability and lead to errors.

.

5. CONCLUSION

In this work, a reliability prediction model is proposed to compute the system reliability of power electronic model capturing the failure mechanism interaction between critical components: wire bond and solder joint. Wire bond and solder joint are important components for thermal, mechanical and electrical connection in IGBT module. The component degradation process is resulted from the stress strength caused by inhomogeneous component structure and temperature amplitude during power cycling. Additionally, failure interaction between component failure modes affects component failure characteristics and is never precisely interpreted. However, most of the existing literatures fail to propose a comprehensive way to deal with IGBT system reliability with the consideration of failure interaction between components. Therefore, the interest of this work is inspired and further proceeded to provide a realistic reliability assessment on PEM.

First, the degradation process of solder joint and wire bond is trigger due to the influence of thermo-mechanical stress. The failure characteristics of solder joint and wire bond are captured via selected PoF model respectively. Dependent to the impact that the effect of thermal strains or temperature amplitude has on critical components many PoF models have been established. To completely capture all the factors contributing to component degradation, component physical dimensions and material properties are taken account. Second, PoF models only estimate the average component lifetime. It does not provide any probabilistic interpretation for reliability assessment. Component lifetime often has variation and follows a certain distribution, which is more of the case in reality. In order to provide realistic reliability analysis, the selected PoF models are converted into probabilistic models. Normal distribution is selected to describe the failure characteristics of component degradation process because fatigue data can

be approximated as normal distribution under random or constant loading condition [37]. Third, the failure interaction between wire bond and solder joint is studied. Wire bond lift-off is treated as the predominant failure mode based upon observed experiments [10] [32] and solder joint delamination is triggered by wire bond degradation process. Increased junction temperature is captured as it is affected by the degradation process of both components. Additionally, both wire bond and solder joint suffered increased thermo-mechanical stress as junction temperature rises. Therefore, with updated junction temperature at each time, the expected component lifetime is estimated. In the end, the system reliability is computed in a series system configuration.

Dataset abstracted from [6] [34] and [42] are mainly used to study the failure characteristics of wire bond and solder joint for the contribution of the increase junction temperature. In addition, 3% change has been used as threshold criteria for initiation phase for solder joint. Nonlinear regression techniques via MINITAB have been used to develop the individual models for wire bond and solder joint respectively. Through Joule’s law, the increased junction temperature is computed based upon the regression models.

Reliability analysis was performed treating the system as a series configuration. System reliability is divided and computed into two phases. In the first phase, only the failure mechanism of wire bond is take account due to its predominance and solder joint not showing any sign of fatigue. The system reliability is only dependent to the failure fatigue of wire bond. The second phase begins when cracks initiated in solder joint. The system reliability is the product of reliability of solder joint and wire bond. Compared to the system reliability with independent assumption, the proposed model indicates earlier failure of the system. This demonstrates the necessity of capturing failure interaction and the acceleration of failure characteristics due the impact of failure interaction. From Figure 18, junction temperature

increases at a faster after 250K cycles. Accordingly, the system reliability has a faster drop after 250K cycles shown in Figure 19. This validates the choice of normal distribution for probabilistic interpretation and the proposal model considering failure interaction between wire bond and solder joint.

In future research, the proposal model needs to be enhanced for various operating conditions incorporating various parameters. This allows more precise prediction on component lifetime for a wider range of applicable situations. Design of experiment can be under taken to find out the effective parameters if dataset is affluent. Comprehensive ANOVA approach can be adopted to accurately model the statistical behavior of V_{CE} and V_{GE} for regression model. Use of Bayesian model could be explored for a better insight into reliability behavior when fatigue data is available.

REFERENCES

[1] H. Wang, "Toward Reliable Power Electronics: Challenges, Design Tools, and Opportunities," *Industrial Electronics Magazine, IEEE* vol. 7.2, pp. 17-26, 2013.

[2] MIL-HDBK-217F, *Reliability Prediction of Electronic Equipment*, 1991. Notice 1 (1992) and Notice 2 (1995).

[3] W. Nelson, *Accelerated testing: statistical models, test plans, and data analysis*. vol. 344. John Wiley & Sons, 2009.

[4] H. Peng, *et al.*, "Reliability and Maintenance Modeling for Systems Subject to Multiple Dependent Competing Failure Processes," *IIE transactions*, vol. 43.1, pp. 12-22, 2010.

[5] H. A. Schafft, Testing and Fabrication of Wire-Bond Electrical Connections-A Comprehensive Survey, *No. NBS-TN-726. NATIONAL BUREAU OF STANDARDS WASHINGTON DC ELECTRONIC TECHNOLOGY DIV*, 1972.

[6] M. Held, *et al*,. "Fast Power Cycling Test for Insulated Gate Bipolar Transistor Modules in Traction Application," *International journal of electronics*, vol. 86.10, pp. 1193-1204, 1999.

[7] A. Micol, *et al*., "An Investigation Into The Reliability of Power Modules Considering Baseplate Solders Thermal Fatigue in Aeronautical Applications," *Microelectronics Reliability,* vol. 49.9, pp. 1370-1374, 2009.

[8] A. Gurmukh and OP. Yadav, "A Unified Model Approach for Solder Joint Life Prediction," in *Reliability and Maintainability Symposium (RAMS), Annual. IEEE*, 2015, pp. 1-7.

[9] R. Amro, *et al*., "Power Cycling With High Temperature Swing of Discrete Components Based On Different Technologies," in *Power Electronics Specialists Conference, IEEE 35th Annual. Vol. 4. IEEE*, 2004, pp. 2593-2598.

[10] L. Yang, *et al*., "Physics-of-Failure Lifetime Prediction Models for Wire Bond Interconnects in Power Electronic Modules," *Device and Materials Reliability, IEEE Transactions on*, vol. 13.1, pp. 9-17, 2013.

[11] SR-332, Reliability Prediction Procedure for Electronic Equipment, *Telcordia,* Issue 2, September 2006.

[12] ITEM Software and ReliaSoft Corporation, RS 490 Course Notes: *Introduction to Standards Based Reliability Prediction and Lambda Predict*, 2006.

[13] Y. Song, and B. Wang, "Survey on reliability of power electronic systems," *Power Electronics, IEEE Transactions on*, vol. 28.1, pp. 591-604, 2013.

[14] W. Huang, "Reliability Analysis Considering Product Performance Degradation," Ph.D. dissertation, Dept. Systems and Industrial Engineering, The University of Arizona, AZ, 2002.

[15] Z. Pan and N. Balakrishnan, "Reliability Modeling Of Degradation of Products With Multiple Performance Characteristics Based on Gamma Processes," *Reliability Engineering & System Safety*, vol. 96.8, pp. 949-957, 2011.

[16] K. Rafiee, *et al*., "Reliability Modeling for Dependent Competing Failure Processes With Changing Degradation Rate." *IIE Transactions,* vol. 46.5, pp. 483-496, 2014.

[17] K. Yang and J. Xue, "Continuous State Reliability Analysis," *Reliability and Maintainability Symposium, 1996 Proceedings. International Symposium on Product Quality and Integrity., Annual. IEEE*, 1996, pp. 251-257.

[18] W. Huang and R.G. Askin, "Reliability Analysis of Electronic Devices With Multiple Competing Failure Modes Involving Performance Aging Degradation," *Quality and Reliability Engineering International,* vol. 19.3, pp. 241-254, 2003.

[19] J.A. Hoeting, *et al.*, "Bayesian Model Averaging: A Tutorial," *Statistical science,* vol. 44.4, pp. 382-401, 1999.

[20] H. Wang and J. Gao, "A Reliability Evaluation Study Based On Competing Failures for Aircraft Engines," *Eksploatacja i Niezawodność*, vol. 16, 2014.

[21] *Microelectronics Reliability: Physics-of-Failure Based Modeling and Lifetime Evaluation*, Jet Propulsion Laboratory, National Aeronautics and Space Administration, Pasadena, CA, 2008.

[22] J. Goehre, *et al.*, "Interface Degradation of Al Heavy Wire Bonds on Power Semiconductors During Active Power Cycling Measured By The Shear Test," *Integrated Power Electronics Systems (CIPS), 2010 6th International Conference on. IEEE*, 2010, pp. 1-6.

[23] J. Onuki, *et al.*, "Reliability of Thick Al Wire Bonds in IGBT Modules for Traction Motor Drives," *Advanced Packaging, IEEE Transactions on*, vol. 23.1, pp. 108-112, 2000.

[24] S. Ramminger, *et al*., "Crack Mechanism in Wire Bonding Joints," *Microelectronics Reliability*, vol. 38.6, pp. 1301-1305, 1998.

[25] J.M. Göhre, “Development And Implementation of An Improved Load Change Test Method for Experimental Determination of The Reliability of Thick Wire Bonds in Power Modules,” Ph.D. dissertation, Dept. Electrical Engineering and computer science, Technical University of Berlin, Berlin, Germany, 2013.

[26] W. Engelmaier, "Solder Joints in Electronics: Design For Reliability," *Design and Reliability of Solders and Solder Interconnections, RK Mahidhara, et. al., ed. The Minerals, Metals & Materials Society,* Warrendale, PA, pp: 9-19, Feb. 1997.

[27] W.W. Lee, *et al.*, "Solder Joint Fatigue Models: Review and Applicability to Chip Scale Packages," *Microelectronics reliability*, vol. 40.2, pp. 231-244, 2000.

[28] H.D. Solomon, "Fatigue of 60/40 solder," *Components, Hybrids, and Manufacturing Technology*, IEEE Transactions on, vol. 9.4, pp. 423-432, 1986.

[29] H.S. Choi, *et al.*, "Prediction of Reliability on Thermoelectric Module Through Accelerated Life Test and Physics-of-Failure." *Electronic Materials Letters*, vol. 7.3, pp. 271-275, 2011.

[30] C.Y. Yin, *et al.*, "A Physics-of-Failure Based Prognostic Method for Power Modules," *Electronics Packaging Technology Conference*, *EPTC 10th. IEEE*, 2008, pp. 1190-1195.

[31] G. Mitic, *et al.*, "Reliability of AlN substrates and Their Solder Joints in IGBT Power Modules," *Microelectronics reliability*, vol. 39.6, pp. 1159-1164, 1999.

[32] T.Y. Hung, *et al.*, "Investigation of Solder Crack Behavior and Fatigue Life of the Power Module on Different Thermal Cycling Period." *Microelectronic Engineering,* vol. 107, pp. 125-129, 2013.

[33] Ciappa, M. "Selected failure mechanisms of modern power modules," *Microelectronics reliability*, vol. 42.4, pp. 653-667, 2002.

[34] A. Morozumi, *et al.*, "Reliability of Power Cycling for IGBT Power Semiconductor Modules," *Industry Applications, IEEE Transactions on*, vol. 39.3, pp. 665-671, 2003.

[35] L.F. Coffin, "A Study of The Effect of Cyclic Thermal Stresses on A Ductile Metal." *American Society of Mechanical Engineers*, vol. 76, pp. 931-950, 1954.

[36] S.S. Manson, *Behavior of Materials Under Conditions of Thermal Stress*, TN 2933: NACA, 1953.

[37] V. Rathod, *et al.*, "Probabilistic Modeling of Fatigue Damage Accumulation for Reliability Prediction," *International Journal of Quality, Statistics, and Reliability*, 2011.

[38] P.H Wirsching and Y.N. Chen, "Considerations of Probability-Based Fatigue Design for Marine Structures," *Marine Structures*, vol. 1.1, pp. 23-45, 1988.

[39] J.M. Bloom and J.C. Ekvall, *Probabilistic Fracture Mechanics and Fatigue Methods: Applications for Structural Design and Maintenance: A Symposium*. No. 798. ASTM International, 1983.

[40] W.F. Wu, *et al.*, "Estimation of Fatigue Damage and Fatigue Life of Components Under Random Loading," *International Journal of Pressure Vessels and Piping*, vol. 72.3, pp. 243-249, 1998.

[41] A. Hamidi, *et al.*, "Reliability and Lifetime Evaluation of Different Wire Bonding Technologies for High Power IGBT Modules," *Microelectronics Reliability*, vol. 39.6, pp. 1153-1158, 1999.

[42] R. Amro, *et al.*, "Power Cycling With High Temperature Swing of Discrete Components Based on Different Technologies," *in PESC 04. 2004 IEEE 35th Annual*. Vol. 4, pp. 2593-2598, 2004.

[43] W. Wu, *et al.*, "Investigation on the Long Term Reliability of Power IGBT Modules," in *Proceedings of the 7th International Symposium on*. IEEE, 1995.

[44] U. Scheuermann, U. "Power Cycling Lifetime of Advanced Power Modules for Different Temperature Swings," in Proc. PCIM PE4. 5, Nürnberg 2002, pp. 59-64.

[45] J. R. Celaya, *et al.*, "Prognostics Approach for Power MOSFET Under Thermal-Stress Aging," in *Proceedings Reliability and Maintainability Symposium 2012 Annual*. IEEE, 2012.

[46] Y. Wang, *et al.*, "*A simulation of Intelligent Power Module under power cycling condition*," *Electronic Packaging Technology (ICEPT), 2014 15th International Conference on*. IEEE, 2014.

[47] Gaiser Precision Bonding Tools, ”Fine-Pitch Capillary,” www.coorstek.com. Web. 09 Sep. 2015.

[48] J. Pang, *et al.*, "Thermal cycling analysis of flip-chip solder joint reliability." *Components and Packaging Technologies, IEEE Transactions on,* vol. 24.4, pp. 705-712, 2001.